

Provided for non-commercial research and education use.  
Not for reproduction, distribution or commercial use.



This article appeared in a journal published by Elsevier. The attached copy is furnished to the author for internal non-commercial research and education use, including for instruction at the authors institution and sharing with colleagues.

Other uses, including reproduction and distribution, or selling or licensing copies, or posting to personal, institutional or third party websites are prohibited.

In most cases authors are permitted to post their version of the article (e.g. in Word or Tex form) to their personal website or institutional repository. Authors requiring further information regarding Elsevier's archiving and manuscript policies are encouraged to visit:

<http://www.elsevier.com/copyright>



Contents lists available at ScienceDirect

## Experimental Eye Research

journal homepage: [www.elsevier.com/locate/yexer](http://www.elsevier.com/locate/yexer)

## Review

## The changing paradigm of outflow resistance generation: Towards synergistic models of the JCT and inner wall endothelium

Darryl R. Overby<sup>a,\*</sup>, W. Daniel Stamer<sup>b</sup>, Mark Johnson<sup>c</sup><sup>a</sup>Tulane University, Department of Biomedical Engineering, New Orleans, LA, USA<sup>b</sup>University of Arizona, Department of Ophthalmology and Vision Science, Tucson, AZ, USA<sup>c</sup>Northwestern University, Department of Biomedical Engineering, Evanston, IL, USA

## ARTICLE INFO

## Article history:

Received 25 July 2008

Accepted in revised form 16 November 2008

Available online 11 December 2008

## Keywords:

trabecular meshwork  
 juxtacanalicular connective tissue  
 Schlemm's canal  
 aqueous humor outflow  
 outflow facility  
 glaucoma

## ABSTRACT

Aqueous humor outflow resistance is the primary determinant of intraocular pressure (IOP), and increased outflow resistance is the basis for elevated IOP associated with glaucoma. Experimental evidence suggests that the bulk of outflow resistance is generated in the vicinity of the inner wall endothelium of Schlemm's canal, its basement membrane and the juxtacanalicular connective tissue (JCT). However, attempts to sort out the contribution of each of these tissues to total outflow resistance have not been successful. Conventional understanding of outflow resistance assumes that the resistance of each tissue strata (i.e., the inner wall endothelium, its basement membrane and JCT) in the outflow pathway adds in series to contribute to total outflow resistance generation. However, this perspective leads to a paradox where the apparent resistances of all tissues in the outflow pathway are much lower than the measured total resistance. To resolve this paradox, we explore synergistic models of outflow resistance generation where hydrodynamic interactions between different tissue strata lead to a total resistance that is greater than the sum of the individual tissue resistances. We closely examine the "funneling" hypothesis that has emerged as a leading synergistic model, and we review the basis of funneling, mechanical and biological requirements for funneling and evidence in support of this hypothesis. We also propose refinements to the funneling model and describe how funneling may relate to segmental variability of aqueous humor outflow patterns observed within the trabecular meshwork. Pressure gradients across the JCT and inner wall endothelium will generate mechanical loads that influence the morphology of these tissues. Because tissue morphology may in turn affect outflow resistance, there exists the potential for a two-way coupling or a "fluid-solid interaction" between outflow hydrodynamics and the mechanical behavior of the inner wall and JCT. Furthermore, the adhesions and tethers between the inner wall and JCT must be physically capable of supporting such loads. We examine the structure and mechanical strength of these adhesions, and provide evidence that these adhesions and tethers are unable to support the full load imposed by the bulk of outflow resistance generation unless a substantial fraction of outflow resistance is generated within the JCT, consistent with the funneling model. This indicates that these attachments between the inner wall and JCT have considerable physiological importance for outflow resistance regulation, by maintaining the proximity between these two tissues to facilitate funneling. Further study is greatly needed to better characterize these important interactions.

© 2008 Elsevier Ltd. All rights reserved.

\* Corresponding author. Department of Bioengineering, Imperial College London, South Kensington Campus, London, SW7 2AZ, UK. Tel.: +44 (0)20 7594 6376; fax: +44 (0)20 7594 9817.

E-mail address: [d.overby@imperial.ac.uk](mailto:d.overby@imperial.ac.uk) (D.R. Overby).

<sup>1</sup> Present address: Imperial College of Science, Technology and Medicine, Department of Bioengineering, London, U.K.

## 1. Introduction

Well over a century has passed since Leber postulated that elevated intraocular pressure (IOP) in glaucoma is caused by increased resistance of aqueous humor drainage from the anterior chamber of the eye (Leber, 1873). Yet still unknown today is how aqueous humor outflow resistance is generated or why it becomes elevated in open-angle glaucoma. All current strategies to treat glaucoma (including normal tension glaucoma) involve reducing

IOP (Collaborative Normal-Tension Glaucoma Study Group, 1998; Kass et al., 2002), but conventional therapies often fail to achieve adequate IOP reduction, leaving surgery as the only option. Glaucoma therapy would be significantly improved by a mechanistic understanding of how outflow resistance is generated and regulated.

The bulk of aqueous humor drainage passes through the conventional outflow pathway (Fig. 1). There is a secondary or “unconventional” pathway for aqueous humor outflow through a uveoscleral or uveovortex route, but this pathway only accounts for 10–35% of total aqueous humor drainage from the human eye (Nilsson, 1997). It does not contribute significantly to normal outflow dynamics in older eyes nor is it believed to contribute to the generation of elevated outflow resistance in glaucoma (discussed in Section 2.2), although modification of uveoscleral outflow is important for glaucoma therapies involving prostaglandin  $F_{2\alpha}$  analogs, as reviewed elsewhere (Johnson and Erickson, 2000).

A significant body of evidence suggests that the bulk of outflow resistance in the normal eye lies in the vicinity of the inner wall endothelium of Schlemm's canal, its basement membrane, and the juxtacanalicular connective tissue (JCT). These same tissues also appear to be involved in generating the elevated outflow resistance associated with glaucoma, evidence that will be reviewed in the first part (Section 2) of this article. Ultrastructural studies, however, have been unable to attribute the bulk of resistance generation to any one of these three tissues, suggesting that outflow resistance may result from a synergistic interaction between the inner wall endothelium, its basement membrane and/or the JCT. A discussion of potential synergistic mechanisms of outflow resistance generation is presented in the second part (Section 3) of this review article. Regardless of the specific mechanism of outflow resistance generation, the inner wall and JCT must be physically capable of supporting the mechanical load arising from the pressure drop across these tissues. This load influences tissue morphology and cellular mechanobiology that in turn influences outflow resistance generation and the mechanical load acting on these tissues. Thus there is the potential for a “fluid-solid” interaction where morphology and resistance generation are intimately coupled through cell and tissue mechanics to regulate IOP. We present these concepts in the third part of this review article (Section 4). Finally, in Section 5 we conclude with recommendations for future work.

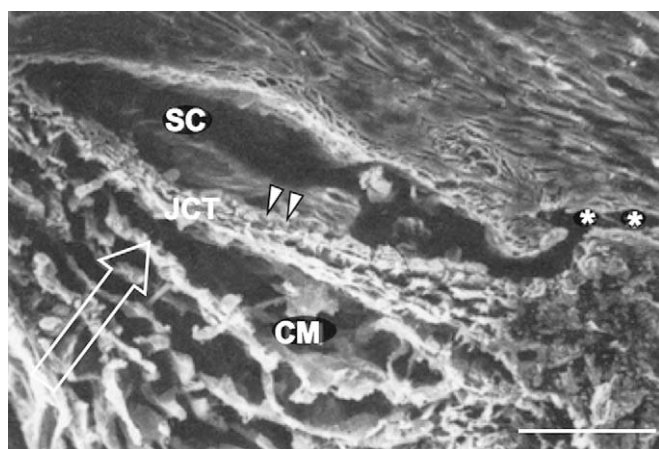


**Fig. 1.** A scanning electron micrograph of the conventional outflow pathway, showing the corneoscleral meshwork (CM), Schlemm's canal (SC), juxtacanalicular connective tissue (JCT), and a collector channel (asterisks). The inner wall of SC is shown (arrowheads), along with the direction of aqueous humor flow (arrow). Scale bar is 50  $\mu$ m. Adapted from Fredo (1993), with permission.

## 2. Conventional views of outflow resistance generation

### 2.1. The conventional aqueous humor outflow system

The aqueous outflow system in the human eye is comprised of the trabecular meshwork, Schlemm's canal, and the collector channels/aqueous veins (Fig. 1). The trabecular meshwork includes the more superficial uveal meshwork, the deeper corneoscleral meshwork, and the juxtacanalicular connective tissue (JCT) adjacent to Schlemm's canal. Schlemm's canal includes the inner wall endothelium, its basement membrane and the canal lumen. Collector channels and aqueous veins connect the canal lumen to the episcleral veins on the surface of the eye.

#### 2.1.1. The trabecular meshwork

The uveal meshwork consists of an irregular netlike structure with cords that interconnect its different layers. The spaces between these cords are so large that little flow resistance is expected in this region (McEwen, 1958), a finding confirmed experimentally by Grant (1963).

The corneoscleral meshwork extends approximately 100  $\mu$ m in the flow-wise direction. It consists of a number of porous sheets, attached to the scleral spur posteriorly and the inner aspects of the peripheral cornea anteriorly. The openings in these sheets decrease progressively in size as the deeper aspects of the meshwork are approached, with a structure like that of a well-designed filter (Bill, 1975).

The deepest aspects of the trabecular meshwork are known as the JCT, also called the endothelial meshwork or cribriform region. This tissue follows the last trabecular beam, and extends to the basement membrane of the inner wall of Schlemm's canal (Fig. 2).

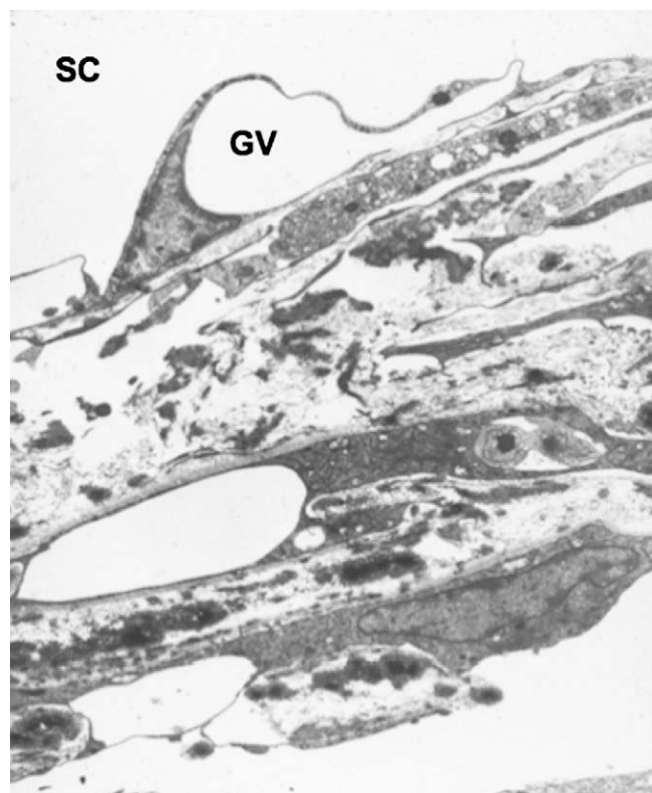


**Fig. 2.** Juxtacanalicular connective tissue adjacent to Schlemm's canal (SC), showing a giant vacuole (GV) at the inner wall. Reproduced from Johnson and Erickson, 2000, with permission.

This region is much less ordered than the corneoscleral meshwork. It is few microns thick at some locations and extends on average 10  $\mu\text{m}$  away from the inner wall endothelium. There are relatively large open spaces in the JCT, especially when it is fixed at pressure, with a porosity that ranges between 30 and 50% (Ten Hulzen and Johnson, 1996). Glycosaminoglycans are found in the JCT, particularly hyaluronic acid, dermatan sulfate and chondroitin sulfate (Knepper et al., 1996a). With age, this region shows an accumulation of extracellular matrix (ECM) structures called plaques (Alvarado et al., 1986; Lütjen-Drecoll et al., 1986). In glaucoma, accumulation of plaque material appears to be accelerated, although the hydrodynamic consequence of this accumulation is likely small (Murphy et al., 1992).

### 2.1.2. Inner wall endothelium of Schlemm's canal

After passing through the tortuous spaces of the JCT, the aqueous humor encounters the endothelial lining of the inner wall of Schlemm's canal (Fig. 3). The inner wall is a confluent layer of elongated cells attached to one another by tight junctions and lying upon a discontinuous basement membrane (Grierson et al., 1978; Gong et al., 1996).

Garron et al., (1958), Holmberg (1959) and Speakman (1959) first described the ultrastructural appearance of inner wall cells. They described an apparently unique feature of many of these inner wall cells, namely structures that were named "giant vacuoles" that appear to be within the cells (Figs. 3 and 4A). These structures (1–10  $\mu\text{m}$  in width, 1–7  $\mu\text{m}$  in height, extending to 20  $\mu\text{m}$  in length) are not intracellular structures. Instead, serial sections show that all of these vacuoles are actually outpouchings of the endothelium caused by the pressure drop across the inner wall endothelium (Inomata et al., 1972).

The wall of these invaginations is very thin, and where the wall is most thin, unique pores are seen to form (Figs. 3 and 5). The majority of these pores (about 75%) are transcellular, although a fraction are located at the border of neighboring cells and are paracellular (Ethier et al., 1998). Inner wall pores do not connect the extracellular fluid with the cytoplasm of the cell, but instead pass from the basal to the apical side of cells where the cell membranes from the inner and outer surfaces of the cell have come together and fused. Pores are thus membrane-lined structures. Not surprisingly, pores usually form on giant vacuoles since it is in this region in which the cell is greatly attenuated and the cytoplasm becomes thin, although pores are occasionally found on flat, thin portions of the inner wall (Inomata et al., 1972).

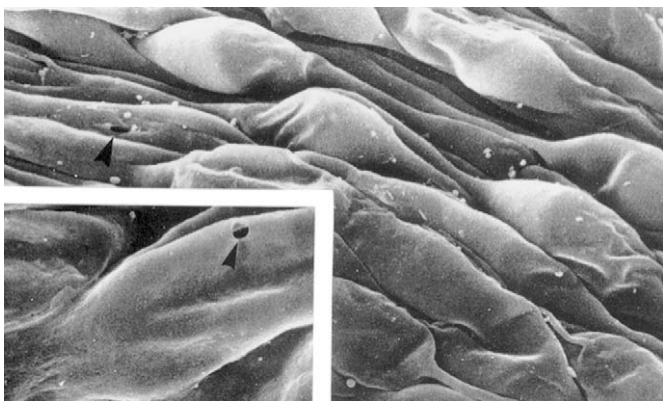


**Fig. 3.** Scanning electron micrograph of the inner wall of Schlemm's canal as seen from the canal lumen. Arrowhead shows a pore and inset shows high magnification image of pore. Adapted with permission from Allingham et al. (1992).

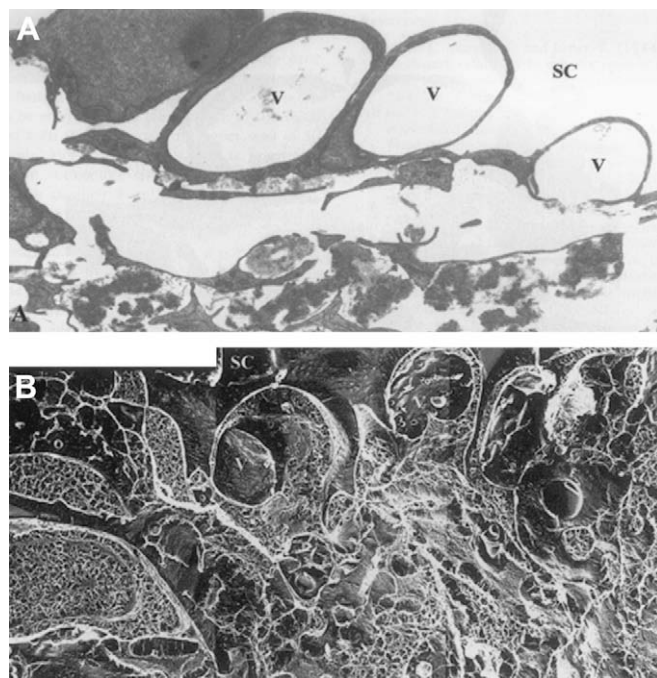


**Fig. 4.** Enucleated human eye fixed by perfusion at 15 mm Hg. (A) Giant vacuoles (V) in the inner wall of Schlemm's canal (SC) in tissue prepared for transmission electron microscopy using conventional methods; notice the large open spaces in the region of the JCT immediately under these giant vacuoles; (B) a similar region as seen in tissue prepared using quick-freeze/deep-etch; notice that while open spaces still exist under the giant vacuoles, a more complex and extensive extracellular matrix is seen. Note that in 4A, open spaces are light, while in 4B, open spaces are dark. (x4860) Reproduced with permission from (Gong et al., 2002).

Inner wall pores usually range in size from 0.1  $\mu\text{m}$  to greater than 3  $\mu\text{m}$  with an average diameter of just under 1  $\mu\text{m}$  (Sit et al., 1997). The density of pores in this endothelium has been estimated to vary between 1000 and 2000 pores/ $\text{mm}^2$  (Kayes, 1967; Bill, 1970; Bill and Svedbergh, 1972; Segawa, 1973; Lee and Grierson, 1975; Svedbergh, 1976), although more recent studies indicate that some of the pores are fixation artifacts and that the density of these pores is less than 1000 pores/ $\text{mm}^2$  in the normal eye (Sit et al., 1997; Ethier et al., 1998).

The aqueous humor is presumed to cross the endothelium of Schlemm's canal by passing through pores. Support for this proposition is found in studies where (i) microparticles up to 1  $\mu\text{m}$  in size pass freely through the conventional outflow pathway to enter Schlemm's canal and (ii) comparisons of the inner wall with other endothelia show that the inner wall has an unusually high measured hydraulic conductivity (see the review by Johnson (2006) for a complete discussion).

### 2.1.3. Schlemm's canal, collector channels and the aqueous veins

After passing through the inner wall endothelium, the aqueous humor enters Schlemm's canal lumen that appears as a highly elongated ellipse in cross-section. Throughout the canal, but especially near collector channels, are septa that bridge between the inner and outer walls of the canal. The proximity of these structures to collector channel ostia suggests that their function may be to prevent complete collapse of the canal lumen and occlusion of collector channel ostia (Bill, 1970; Hoffman and Dumitrescu, 1971; Johnson and Kamm, 1983).

After entering the canal, aqueous humor travels circumferentially around the eye until it reaches one of roughly 30 collector channel ostia along the outer wall of Schlemm's canal. The

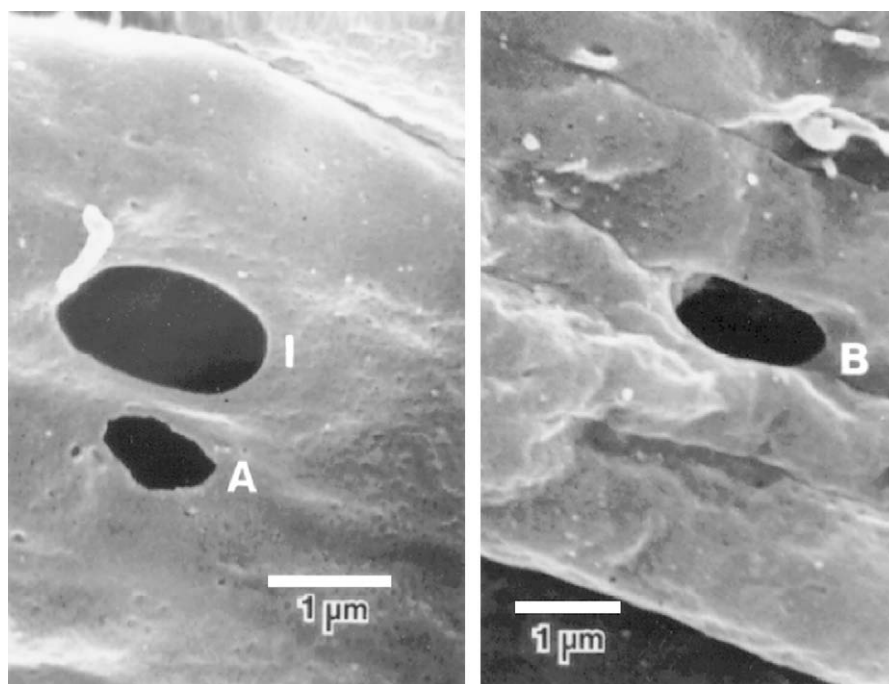


**Fig. 5.** Pores of the inner wall endothelium. Left: Intracellular pores (I) and artificial pore (A); Right: intercellular or border (B) pore. Reproduced with permission from (Ethier et al., 1998).

collector channels are tens of microns in diameter (Dvorak-Theobald, 1934; Rohen and Rentsch, 1968; Tripathi, 1974). Aqueous humor flowing through these collector channels ultimately drains into the episcleral venous system.

## 2.2. Sites of minor outflow resistance generation

### 2.2.1. Resistance generated within the uveal and corneoscleral meshworks

The uveal and corneoscleral meshworks are very porous structures with numerous openings that range in size from 25–75  $\mu\text{m}$  in the proximal regions of the uveal meshwork to 2–15  $\mu\text{m}$  in the deeper layers of the corneoscleral meshwork (Tripathi, 1974). According to Poiseuille's law, a single channel 100  $\mu\text{m}$  long (the thickness of the trabecular meshwork in the flow-wise direction) and 20  $\mu\text{m}$  in diameter can carry the entire aqueous humor outflow (2  $\mu\text{L}/\text{min}$ ) with a pressure drop of 5 mm Hg, allowing the conclusion that the flow resistance in these regions is negligible (McEwen, 1958). Grant (1963) provided experimental support for this conclusion by surgically removing the proximal aspects of these tissues in enucleated human eyes and demonstrating no effect on outflow resistance.

### 2.2.2. Resistance generated within Schlemm's canal

While Schlemm's canal is open at low intraocular pressure, Johnson and Grant (1973) showed that the trabecular meshwork expands and the canal lumen collapses as the intraocular pressure is increased (Fig. 6). While the distance between the inner wall and outer walls of the canal at low intraocular pressure is much too large to generate a significant outflow resistance (Moses, 1979), collapse of Schlemm's canal to a size of a few microns or less at higher IOP has led some to speculate that this might be a cause of primary open-angle glaucoma (Nesterov, 1970).

However, Johnson and Kamm (1983) pointed out that collapse of the canal does not generate a flow resistance nearly as high as that of a glaucomatous eye (Brubaker, 1975; Van Buskirk, 1976; Moses, 1977). Thus, while collapse of the canal will likely make

a glaucomatous condition worse, it will not, in and of itself, cause glaucoma.

### 2.2.3. Resistance in collector channels and aqueous veins

The collector channels and aqueous veins are relatively large vessels that are tens of microns in diameter (Dvorak-Theobald, 1934; Rohen and Rentsch, 1968; Tripathi, 1974). Use of Poiseuille's law leads to the conclusion that these vessels generate negligible flow resistance (Rosenquist et al., 1989).

However, the experimental evidence is mixed. While Mäepea and Bill (1989, 1992) measured the pressure in Schlemm's canal of monkey eyes and found that the pressure in the canal differed little from that in the aqueous veins, a different conclusion was reached from studies in which a trabeculectomy was used in enucleated human eyes to eliminate all flow resistance proximal to the collector channels and aqueous veins. These studies show that at least 25% of outflow resistance remains after this procedure, in sharp contrast to what would have been predicted based on the results of the Mäepea and Bill experiments (Grant, 1958, 1963; Ellingsen and Grant, 1972; Van Buskirk and Grant, 1973; Peterson and Jocson, 1974; Van Buskirk, 1977). More recently, the relative high IOP after the surgical use of the Trabectome (Minckler et al., 2005) supports the existence of considerable flow resistance distal to Schlemm's canal in human eyes.

While the discrepancy between these studies has not been resolved, its importance has been somewhat diminished by the observation that these vessels are not likely to be responsible for the elevated flow resistance characteristic of glaucoma (Johnson, 2006). An early study by Grant (1963) showed that a trabeculectomy eliminated all of the elevated glaucomatous outflow resistance in 8 glaucomatous eyes, indicating that in primary open-angle glaucoma the outflow obstruction lies proximal to the collector channels and aqueous veins. Furthermore, it is difficult to explain the efficacy of laser trabeculoplasty (LTP) in reducing outflow resistance in glaucomatous eyes if the elevated resistance in glaucoma is generated primarily in the collector channels and/or aqueous veins (Wise and Witter, 1979). These considerations suggest that, at least

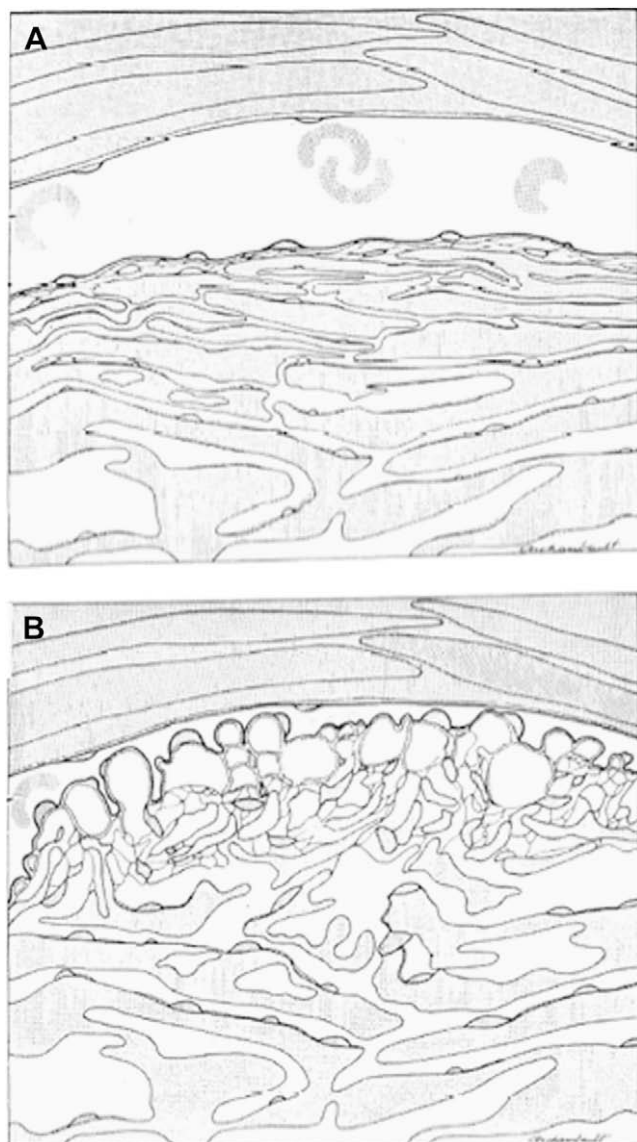


**Fig. 6.** Schematic of changing configuration of inner wall endothelium, trabecular meshwork and Schlemm's canal at low (A) and high (B) perfusion pressure. Reproduced with permission from (Johnstone and Grant, 1973).

in most cases of glaucoma, the elevated outflow resistance associated with this disease has its origins in changes in the tissues upstream of the collector channels and aqueous veins, although further work is needed to determine the resistance generated by these downstream vessels and whether they contribute to elevated resistance in glaucoma.

### 2.3. Sites of significant outflow resistance generation

Experimental evidence supports the conclusion that the source of normal outflow resistance as well as the source of increased outflow resistance in glaucoma is attributable to the inner wall endothelium, its basement membrane, JCT, or some combination of all three of these tissues. In support of this conclusion, Mäepea and Bill (1989, 1992) used micro-cannulation to measure pressure at various points throughout the trabecular meshwork, Schlemm's canal and episcleral veins in anesthetized monkeys. Their data revealed that the bulk of the pressure drop across the outflow pathway lies within 14  $\mu\text{m}$  upstream of the inner wall endothelium

(Mäepea and Bill, 1992), although the spatial resolution of their measurements have recently come into question (Johnson, 2006). It is also noteworthy that, while the Mäepea and Bill experiment localizes the bulk of outflow resistance to the immediate vicinity of the JCT and/or inner wall endothelium of the normal eye, no such experiment has yet been done on glaucomatous eyes.

Pharmacological evidence also supports the conclusion that a significant fraction of aqueous humor outflow resistance is generated at or near the inner wall endothelium of Schlemm's canal. When proteolytic enzymes ( $\alpha$ -chymotrypsin; (Hamanaka and Bill, 1988)) or chelating agents (EDTA, EGTA: (Bill et al., 1980; Hamanaka and Bill, 1987)) are perfused through the outflow pathway of live primates, ruptures of the inner wall endothelium are produced that significantly affect outflow resistance, suggesting that these agents decrease outflow resistance by increasing the hydraulic conductivity of the inner wall endothelium. Alternatively, the ruptures created in the inner wall endothelium may affect the extracellular matrix in the basement membrane or JCT near these ruptures, and thereby decrease outflow resistance.

#### 2.3.1. The inner wall basement membrane as a source of outflow resistance

By analogy to other basement membranes in the body, the inner wall basement membrane has the potential to generate a significant portion of outflow resistance. Indeed, nearly all of outflow resistance could be attributed to a basement membrane like that of the renal glomerulus (see review by Johnson (2006)). However, the inner wall basement membrane is patchy and discontinuous (Grierson et al., 1978; Gong et al., 1996), which would appear to substantially limit the resistance that can be generated by this tissue. The discontinuities in the basement membrane have been confirmed using several forms of tissue processing for electron microscopy (Brilakis and Johnson, 2001) including quick-freeze/deep-etch (Gong et al., 2002). It is not clear what causes the discontinuities in the basement membrane, but these may be related to the flow of aqueous humor into Schlemm's canal (Buller and Johnson, 1994) because the outer wall basement membrane has been observed to be more continuous (Grierson et al., 1978).

#### 2.3.2. The JCT as a source of outflow resistance

As seen using conventional transmission electron microscopy, the JCT contains micron-sized open spaces that appear devoid of ECM ultrastructure and may represent tortuous pathways for flow to reach the inner wall. Image analysis of these open spaces combined with porous media theory generated predictions of JCT resistance that failed to account for more than a few percent of total outflow resistance (Seiler and Wollensak, 1985; Ethier et al., 1986; Ten Hulzen and Johnson, 1996). Simply put, the open spaces were too large to generate significant resistance unless these were filled with an unobserved ECM gel (Ethier et al., 1986). Importantly, if these spaces were assumed to be filled with glycosaminoglycans (GAGs) at physiologic concentrations, the predicted flow resistance of this porous medium was consistent with the measured values of aqueous outflow resistance (Ethier et al., 1986). This suggested that GAGs – known to collapse when the tissue is dehydrated and embedded within hydrophobic resin for conventional transmission electron microscopy (TEM) (Hascall and Hascall, 1982) – may be involved in resistance generation but are rendered “invisible” by conventional processing for TEM.

To visualize the fine ultrastructure of the JCT in normal human eyes, Gong et al. (2002) used quick-freeze/deep-etch (QF/DE) electron microscopy, a technique that better preserves native ECM ultrastructure. QF/DE revealed a much more intricate and complex ECM as compared to conventional TEM, but open spaces devoid of matrix that were similar in size to those observed with

conventional methods were still observed within the JCT (Fig. 4B) (Gong et al., 2002). These data suggest that either the JCT may not contribute significantly to outflow resistance generation in the normal eye or that QF/DE is still not sensitive enough to visualize the fine ECM ultrastructure involved in resistance generation. In support of the latter point, a QF/DE study of vitreous humor revealed relatively little hyaluronic acid compared to collagen, despite hyaluronic acid being present in this tissue at nearly 10-fold higher concentrations (Bos et al., 2001).

The extracellular matrix within the JCT has long been considered a potential source of outflow resistance generation. Proteoglycans and GAGs contribute to interstitial flow resistance in many tissues (Levick, 1987), and Bárány first identified that aqueous humor outflow resistance may be decreased by nearly 50% in bovine eyes after perfusion with testicular hyaluronidase (Bárány and Scotchbrook, 1954). Similar findings in canine (Van Buskirk and Brett, 1978), guinea pig and rabbit eyes (Melton and DeVille, 1960; Knepper et al., 1984) have led to the general concept that a GAG-rich barrier serves as a principle resistive element to aqueous humor outflow.

In monkey and human eyes, the situation is less clear. In live monkeys, Sawaguchi et al. (1992) reported that chondroitinase ABC lowered IOP; however, Hubbard et al. (1997) reported that neither *Streptomyces hyaluronidase* nor chondroitinase ABC has any effect upon outflow resistance. There is no clear effect of testicular hyaluronidase on enucleated eye bank human eyes (Pedler, 1956; Grant, 1963). A recent study in human organ cultured eyes (Keller et al., 2008) showed that biochemical inhibition of GAG elongation or sulfation decreases outflow resistance, supporting a role of GAGs in generating outflow resistance in human eyes. However, in that same study, GAGases had no effect on outflow facility in these human eyes, in spite of finding a resistance-decreasing effect in porcine organ culture eyes. Thus it remains unclear whether GAGs contribute to outflow resistance generation in the human eye, or whether accumulation or depletion of specific GAG subtypes may be involved in glaucoma (Knepper et al., 1996a,b).

In summary, it remains unclear what fraction of total resistance is attributable to the JCT and how ECM or specific ECM molecules might be involved in generation of this resistance.

### 2.3.3. The inner wall endothelium as a source of outflow resistance

The majority of aqueous humor likely crosses the inner wall through pores, and morphometric analysis of these pores can be used to estimate the resistance generated by the inner wall endothelium. Taking this approach, Bill and Svedbergh (1972) calculated the flow resistance attributable to inner wall pores in human eyes using Sampson's law from theoretical hydrodynamics (Happel and Brenner, 1983):

$$\frac{24 \mu}{d^3 n A} \quad (1)$$

where  $\mu$  is aqueous humor viscosity,  $d$  and  $n$  represent the diameter and density of inner wall pores respectively, and  $A$  is the inner wall area. Results from this study suggested that the inner wall itself could account for at most 10% of normal physiologic outflow resistance (Bill and Svedbergh, 1972), and similar conclusions were reported from other studies (Svedbergh, 1976; Eriksson and Svedbergh, 1980; Moseley et al., 1983). However, such a conclusion rests on the assumption that all visualized pores are present and functional *in vivo*, which based upon current understanding may not be the case.

When the inner wall is fixed with glutaraldehyde while being perfused, the density of pores increases in proportion to the volume of fixative passing through the outflow pathway (Sit et al., 1997;

Ethier et al., 1998; Johnson et al., 2002). Accounting for this artifact and extrapolating to zero fixative volume suggests that the inner wall pore density prior to fixation may be as low as 600–900 pores/mm<sup>2</sup> (Sit et al., 1997), compared to the values of 1400–1800 pores/mm<sup>2</sup> as previously reported (Bill and Svedbergh, 1972; Allingham et al., 1992). Importantly, a recent study (Johnson et al., 2002) has concluded that the pore density is significantly reduced in glaucomatous eyes, confirming an earlier report (Allingham et al., 1992). These findings suggest that inner wall pores may contribute to the pathologic increase in outflow resistance experienced in primary open-angle glaucoma.

It remains unclear exactly how pores contribute to outflow resistance generation. As discussed in more detail Section 3.3, a number of studies have failed to find a correlation between pore density and outflow resistance. On the contrary, pore density and size have been reported to increase in some instances where outflow resistance actually increases, such as with increasing intraocular pressure (Grierson and Lee, 1975a, 1978; Lee and Grierson, 1975; Svedbergh, 1976) and during fixation (Ethier et al., 1998; Johnson et al., 2002; Sit et al., 1997), but these studies cannot rule out the possibility that the resistance increase is caused elsewhere in the outflow pathway (e.g., canal collapse or fixative-induced changes in ECM). This lack of correlation may have to do with the confounding effects of fixation on pore density, or may indicate that outflow resistance depends on more factors than just pore density, as we suggest below.

Results from several perfusion studies suggest that the resistance contribution of the inner wall may be larger than that estimated based upon pore morphometry. Several studies have demonstrated a decrease in outflow resistance that exceeds 10% in response to endothelial disruption of the inner wall using EDTA (Hamanaka and Bill, 1987),  $\alpha$ -chymotrypsin (Hamanaka and Bill, 1988), or cytochalasin-D (Johnson, 1997).

In summary, there is significant evidence to suggest that the inner wall endothelium is involved in outflow resistance generation, but exactly how much resistance can be attributed to the endothelium and to the pores themselves remains uncertain.

### 2.4. The paradox of outflow resistance generation

As reviewed above, there is strong evidence to support that the locus of outflow resistance generation lies in the vicinity of the inner wall, its basement membrane and the JCT. However, physiological, pharmacological and morphometric studies have been largely unable to attribute the bulk of resistance to any one of these tissues, partly because most studies are unable to isolate the effect of these different structures. Thus, while it is widely accepted that the inner wall and JCT are important for outflow resistance generation, current data are unable to attribute the bulk of resistance to any single tissue. This is the paradox of outflow resistance generation. In the following Section 3, we explore synergistic models that may resolve this paradox.

## 3. Synergistic models of outflow resistance generation

In developing hydrodynamic models of outflow resistance generation, a general assumption has been that the resistance of each tissue stratum adds in series to contribute to total outflow resistance. However, this perspective leads to a paradox because the apparent flow resistances of all tissues in the circuit are much lower than the measured total outflow resistance. While one resolution of this paradox would be to allow that one or more tissues has a higher flow resistance than would be estimated based upon the apparent size of the flow passages seen in histological preparations, another resolution can be found in using a synergistic

model of outflow resistance. In such a model, hydrodynamic interactions between different tissue strata (i.e., the inner wall endothelium, basement membrane and JCT) may lead to a resistance that is larger than the resistance these tissues would generate without their proximity to one another. Support for this view is provided from data showing that pharmacologic disruption of the inner wall (e.g., by EDTA or cytochalasin-D) decreases outflow resistance by more than can be attributed to the inner wall based upon pore morphometry alone (Hamanaka and Bill, 1987, 1988; Johnson, 1997; Bahler et al., 2004).

In Section 3.1, we describe the “funneling” model that has emerged as the primary synergistic model of outflow resistance generation in which pores in the inner wall affect flow patterns in the JCT, and in Section 3.2 we describe revisions to the funneling model that include the effects of giant vacuoles and the basement membrane. In Section 3.3 we review evidence relating to the support for the funneling model. Finally, in Section 3.4, we review how the funneling model may relate to segmental flow in which larger scale inhomogeneities are seen in flow patterns through the outflow network.

### 3.1. The funneling model

As indicated above, the best evidence now indicates that aqueous humor crosses the endothelium of Schlemm’s canal through micron-sized pores in an otherwise continuous and relatively impermeable endothelial monolayer. The fairly wide pore separation distance (20–30 μm) implies that flow towards these pores must be non-uniform since the flow patterns must “funnel” or converge as flow approaches a pore. Since the JCT is immediately upstream of these pores, the flow patterns in the JCT must also be non-uniform (see Fig. 7A).

This non-uniform flow decreases the effective area available for flow through the JCT that in turn increases the effective hydraulic resistance of this region. Modeling the JCT as a porous medium and using Darcy’s law, Johnson et al. (1992) found that funneling increases the JCT flow resistance by a factor  $E$ :

$$E = 1 + \frac{1}{4 n a L} \quad (2)$$

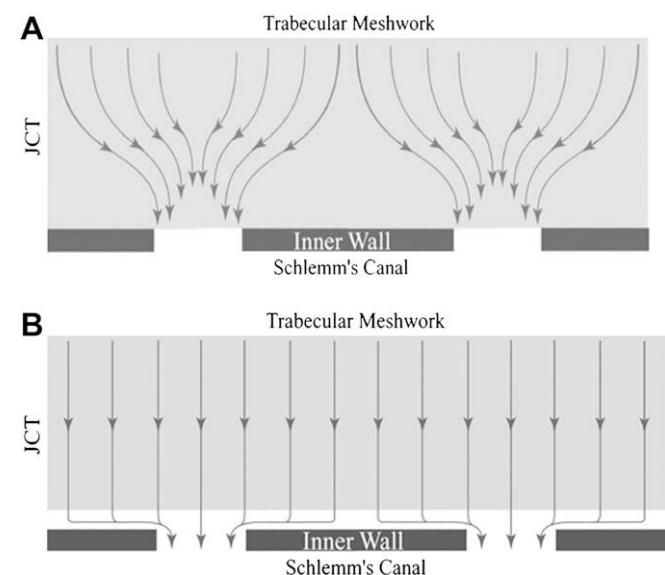


Fig. 7. Schematic showing funneling phenomenon. (A) Flow distribution with inner wall cells attached to substratum; (B) uniform flow that results when these attachments are broken. Reproduced with permission from (Overby et al., 2002).

where  $n$  is the pore density,  $2a$  is the pore diameter and  $L$  is the thickness of the JCT. Using parameter values appropriate for a non-glaucomatous human eye ( $n = 1500$  pores/mm<sup>2</sup>;  $2a = 1$  μm;  $L = 10$  μm), Johnson et al. predicted a 30-fold increase in JCT resistance attributable to funneling (Johnson et al., 1992).

### 3.2. Revising the funneling model

The funneling model explains how breaks in the inner wall endothelium caused by pharmacological agents can have much larger effect on outflow resistance than would be explained based on the flow resistance of the cellular lining alone, since such breaks would presumably eliminate the funneling effect and lead to a more uniform flow pattern in the JCT (Fig. 7B). However, the effects of inner wall breaks on outflow resistance are somewhat more modest than the 30-fold prediction of the funneling model. For example, in live monkeys, EDTA leads on average to roughly an 85% decrease in outflow resistance (Bill et al., 1980), that is consistent with a value of  $E$  of approximately 6.

Most pores are associated with giant vacuoles (Inomata et al., 1972), and these vacuoles open on their basal aspect to the JCT. The larger basal opening of the giant vacuole increases the funneling area compared to a pore that is not associated with a giant vacuole. Similar considerations apply to the discontinuities in the basement membrane underlying the Schlemm’s canal cells. Thus, the proper length scale in Equation (2) should be the vacuole radius ( $R$ ), or the basement membrane discontinuity size, rather than the pore radius  $a$ . However, the density of openings appropriate for use in the model is not the density of giant vacuoles or basement membrane discontinuities but instead remains the pore density,  $n$ , since no fluid will pass through either of these structures unless it also has a pore to allow the fluid to cross the endothelial cell layer.

This revision to the model yields:

$$E = 1 + \frac{1}{4 n R L} \quad (3)$$

As indicated above, estimates of pore density now suggest that this value is 1000 pores/mm<sup>2</sup> or less. Grierson and Lee (1977) characterized inner wall vacuoles as prolate ellipsoids with an average length of 5.2 μm and a width of 2.4 μm, yielding an effective circular radius of approximately 1.8 μm. Using these values in Equation (3) yields a value for  $E$  of approximately 15, still significantly higher than would be estimated based upon experimental studies. This suggests that the funneling area is larger than that of giant vacuoles, and may indicate that the discontinuities in the basement membrane may control this parameter, but unfortunately the average size of basement membrane discontinuities has not been reported.

### 3.3. Support for the funneling model

While studying the resistance-decreasing effect of H-7 (1-5-isoquinolinylnyl-sulfonyl-2-methylpiperazine) in live monkey eyes, Sabanay et al. (2000) reported that perfusion with H-7 (300 μM) caused a redistribution of a colloidal gold tracer that they used in their experiments from sparse foci occupying 10–20% of the inner wall length in untreated eyes to a more uniform tracer labeling along >80% of the inner wall (Fig. 8). The former distribution is what would be expected based upon the funneling effect while the latter suggests that H-7 eliminates funneling.

The change from a punctate to a uniform tracer decoration pattern coincided with nearly a two-fold decrease in outflow resistance without a perceptible change in endothelial continuity (Sabanay et al., 2000). One caveat is that the authors preserved the duration – rather

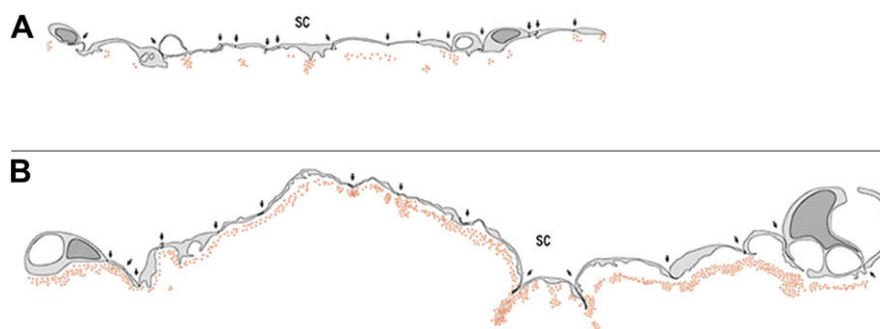


**Fig. 8.** Schematic of inner wall endothelium of monkey eye perfused with colloidal gold. (A) control eye; (B) eye perfused with H-7. Each panel shows an equivalent number of endothelial cells. Reproduced with permission from (Sabanay et al., 2000).

than the volume – of tracer perfusion between paired eyes, such that H-7 treated eyes received roughly twice the volume of tracer compared to contralateral control eyes. It is not clear to what extent the greater number of tracer particles might contribute to the more uniform tracer distribution in H-7 treated eyes.

The decreasing outflow resistance induced by H-7 is associated with morphologic changes consistent with separation between the inner wall and JCT. Following H-7 treatment in live monkeys, Sabanay et al. (2000) reported “relaxed areas” with JCT expansion and protrusion of the inner wall into the lumen of Schlemm’s canal (Fig. 9) without a loss of inner wall cell continuity or disruption of inter-cellular junctions. Importantly, the effects of H-7 upon outflow resistance were reversible 2.5 h after drug removal (Tian et al., 1998), coinciding with a return of inner wall/JCT morphology towards normal (Sabanay et al., 2004).

These results suggest that connectivity between JCT and inner wall cells may be an important regulator of the funneling effect. Support for this conclusion is found in studies of the “washout” effect. “Washout” is the progressive decrease in outflow resistance that occurs during prolonged anterior chamber perfusion in many species (e.g., bovine (Bárány, 1953), porcine (Yan et al., 1991), canine (Van Buskirk and Brett, 1978) and living monkey eyes (Kiland et al.,

2005)), but does not occur in human eyes (Erickson-Lamy et al., 1990). Washout was originally attributed to a “washing out” of GAGs from the outflow pathway during perfusion (Bárány and Scotchbrook, 1954; Bárány and Woodin, 1955; Melton and DeVile, 1960; Van Buskirk and Brett, 1978), but such an idea is inconsistent with biochemical studies that failed to detect a significant removal of either hyaluronic acid (Knepper et al., 1984) or sulfated proteoglycans (Johnson et al., 1993) during washout.

Overby et al. (2002) postulated that washout might be due to a loss of mechanical tethering between the inner wall endothelium and the JCT. Physical separation between the inner wall and JCT would eliminate the funneling interaction and decrease outflow resistance by removing the hydrodynamic influence of the inner wall and allowing uniform outflow through the JCT (see Fig. 7B) (Overby et al., 2002). This hypothesis suggested that washout might be reversible if the inner wall endothelium and JCT were allowed to reattach to one another.

The tethering hypothesis was tested in bovine eyes by halting perfusions and reducing IOP to 0 mm Hg after washout for 1–2.5 h and examining the resulting effect on outflow resistance. Results showed that washout under such conditions was reversible and that the extent of washout reversal correlated with the extent of separation between the inner wall and JCT (Overby et al., 2002; Scott et al., 2007). Sabanay et al. (2004) confirmed these results in live monkey eyes. It is worthwhile pointing out that the hour-long periods necessary for washout reversal are inconsistent with the day-long periods required for GAG biosynthesis in the trabecular meshwork (Acott et al., 1988), suggesting that GAG recovery could not explain the washout reversal effect.

While these data provide strong support for the funneling hypothesis, evidence of an inverse correlation between inner wall pore density and outflow resistance, as is predicted by Equation (2), is equivocal. In studies in which both pore density and outflow resistance have been measured, most studies have failed to find a correlation between these variables (Sit et al., 1997; Ethier and Coloma, 1999; Ethier et al., 1999, 2006), although the study by Allingham et al. (1992) is a notable exception (this could be due to an artifact because fixation volume was not accounted for), and Johnson et al. (2002) found pore density to be reduced in glaucomatous eyes. However, in cases where pharmacologic agents were used to decrease outflow resistance, several studies have reported an increased pore density (Grierson et al., 1979; Bill et al., 1980; Moseley et al., 1983; Ethier et al., 2006), consistent with predictions of the funneling model.

Taken together, while there is substantial support for hydrodynamic interactions between the JCT and the inner wall endothelium, a detailed verification of the predictions of the funneling model have not yet been obtained. Such hydrodynamic interactions may also occur at larger length scales in the outflow pathway, as discussed in the next section.

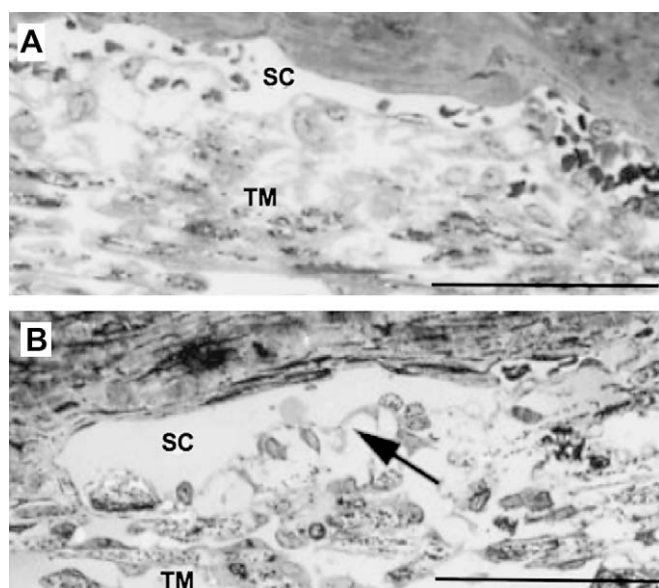


**Fig. 9.** Light micrographs of trabecular meshwork (TM) and Schlemm’s canal (SC) in monkey eyes treated with H-7 (B) or vehicle (A). The JCT and intercellular spaces are extended following H-7 (arrow in B). Bars are 50  $\mu$ m. Adapted from Sabanay et al. (2000), with permission.

### 3.4. Relationship to segmental flow

Aqueous humor outflow has been reported to be non-uniform or “segmental” as observed from the distribution of pigment granules about the trabecular meshwork (Gottanka et al., 2001) and from tracer studies using cationic ferritin (de Kater et al., 1989; Ethier and Chan, 2001; Hann et al., 2005), horse radish peroxidase (MacRae and Sears, 1970), and fluorescent microspheres (Battista et al., 2008; Lu et al., 2008) (see Fig. 10). These flow patterns vary over dimensions ranging from hundreds of micrometers to millimeters such that outflow passes through only a fraction of the available area of the inner wall and JCT.

Gong, Overby and colleagues postulated that segmental flow might be a function of regional variations in funneling due to variable tethering of the inner wall to the JCT (Overby et al., 2006; Battista et al., 2008; Lu et al., 2008). Thus, flow would preferentially go to those regions of the outflow network where the inner wall endothelium has separated from its substratum. They referred to this flow area as the “effective filtration area”. To examine this hypothesis, they perfused fluorescent tracer microspheres through the outflow pathway and measured the “effective filtration length” (the one-dimensional equivalent to effective filtration area, as seen with confocal sectioning) under conditions of varying outflow resistance and determined the relationship between effective filtration length and outflow resistance.

They (Lu et al., 2008) perfused enucleated bovine eyes with fluorescent tracer microspheres (0.5  $\mu\text{m}$  diameter) with or without 50  $\mu\text{M}$  Y-27632, an inhibitor of rho kinase and cell contractility (Uehata et al., 1997; Ishizaki et al., 2000). Results show a redistribution of flow patterns from a segmental or punctate distribution localized near collector channel ostia in control eyes to a more uniform pattern following Y-27632 (Fig. 10) with a 3-fold increase in the percent effective filtration length. Importantly, the observed increase in effective filtration length was associated with increased inner wall separation from the JCT.

The relative decrease in outflow resistance following Y-27632 or sham-treatment was found to correlate significantly with both the percent effective filtration length and the fraction of inner wall length exhibiting separation from the JCT (Lu et al., 2008). Conversely, in studies in which outflow resistance increased following elevated IOP, a decrease in effective filtration length was reported with outflow patterns becoming more focused towards collector channel ostia (Battista et al., 2008). These data support the hypothesis that segmental flow in the outflow pathway may influence outflow resistance generation with outflow patterns sensitive to local separation between the inner wall and JCT.

Significantly, it appears that both funneling and segmental outflow depend on the integrity of the attachment of the inner wall endothelium to the JCT. In the next section, we explore this mechanical coupling.

## 4. Mechanical coupling between the inner wall and JCT

The pressure gradient across the JCT and inner wall endothelium generates mechanical loads on these tissues. With increasing IOP, mechanical forces impose significant stresses, leading to expansion of the JCT, increased numbers of giant vacuoles, and distension of the JCT and inner wall into Schlemm's canal lumen. Due to these forces, a number of mechanical considerations arise. Because tissue morphology may in turn affect outflow resistance, there exists the potential for a coupling or a “fluid-solid interaction” between outflow hydrodynamics and the mechanical behavior of the inner wall and JCT. In addition, inner wall cells and the attachments between the inner wall, its basement membrane and JCT must be physically capable of supporting the mechanical load acting on this

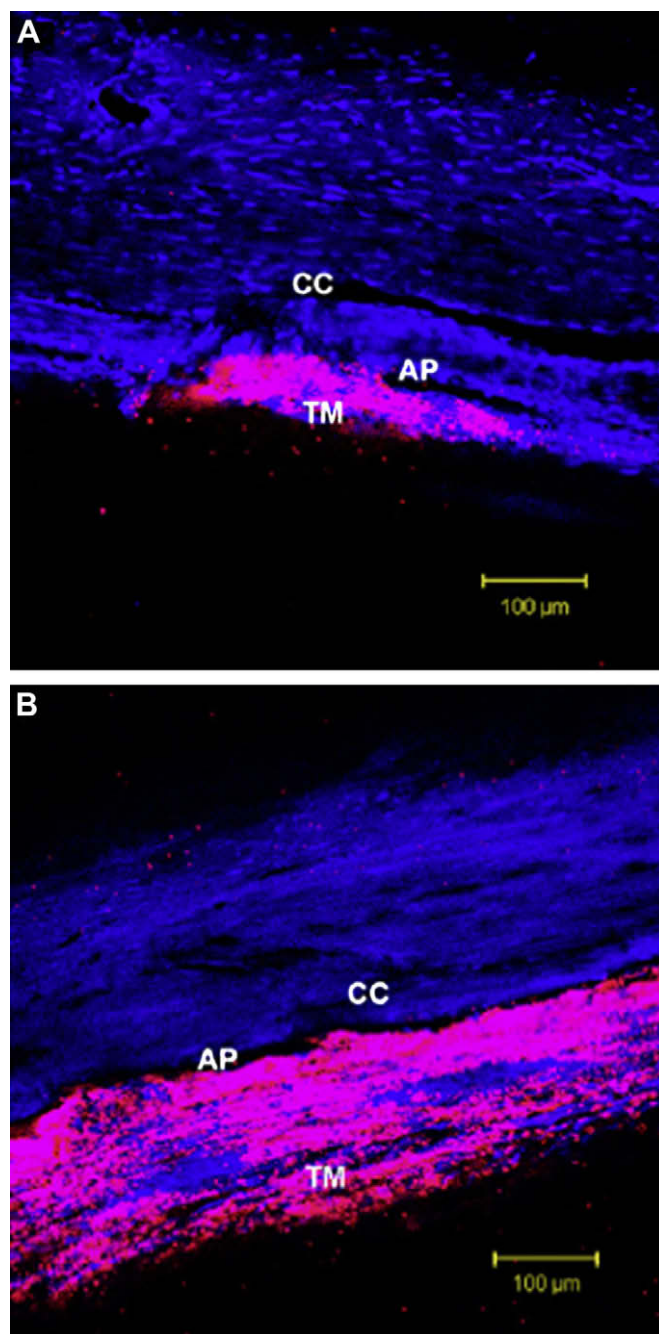


**Fig. 10.** Confocal microscopy of fluorescent tracer patterns within the trabecular meshwork (TM) of bovine eyes and along the inner wall of the aqueous plexus (AP; the bovine equivalent to Schlemm's canal). The tracer distribution (pink) was more segmental in control eyes (A), and tended to concentrate near the ostia of collector channels (CC), while in Y-27 treated eyes (B) the tracer distribution was more uniform along the inner wall. Nuclear background stain is shown in blue. Adapted with permission from Lu et al. (2008).

endothelium. In this section, we review the mechanical behavior of the inner wall and JCT, focusing on the mechanical and biological interactions between these tissues that influence the generation of outflow resistance.

### 4.1. Role of mechanical tethering between the inner wall and JCT

Johnstone and Grant (1973) were the first to describe the morphologic changes in the inner wall and JCT occurring with

increasing IOP in enucleated human and live primate eyes. At low IOP, the inner wall appeared flat and in close proximity to a thin JCT with few giant vacuoles, while Schlemm's canal was wide open. As IOP was increased, the JCT expanded, while the inner wall became highly distended with numerous giant vacuoles and narrowing of Schlemm's canal (Fig. 6). Similar findings were reported in other studies (Grierson and Lee, 1974, 1975b,c). Importantly, these morphological changes were proposed to facilitate fluid outflow and passage of particulates (e.g., pigment, cellular debris) at positive pressure, while also functioning as a one-way valve preventing reflux of blood cells and plasma into the anterior chamber when IOP was reduced below episcleral venous pressure (Johnstone and Grant, 1973).

#### 4.1.1. Cell–cell tethers

Ultrastructural examination by Johnstone (1979) revealed cytoplasmic processes extending from the inner wall endothelium into the subendothelial space, making appositional contact with the processes extending from JCT cells. These processes were proposed to provide an anchoring or tethering support to the inner wall to compensate for the discontinuous basement membrane underlying the inner wall endothelium (Grierson et al., 1978). With increasing IOP, inner wall cell nuclei transitioned from a rounded, lobulated shape into a fusiform shape tapering towards the processes, indicating intercellular force transmission to the nucleus, likely through the cytoskeleton as observed *in vitro* (Maniotis et al., 1997). The JCT cells in turn are tethered via processes to cells lining the corneoscleral trabeculae (Grierson and Lee, 1975b), creating a mechanically continuous network for distributing and transmitting forces to upstream supporting elements.

Grierson et al. (1978) examined the nature of the associations between the cells of the inner wall and JCT, and identified 5 types of appositional contacts between these cells (Fig. 11), including process-to-process, tongue-in-groove and process-to-cell contacts. In rhesus monkey eyes fixed at 15 mm Hg, process-to-process

connections (type 4 in Fig. 11) were most prevalent (~40%), followed by process-to-cell (~30% type 5, ~25% type 2), but surprisingly these contacts only rarely contained gap or maculae adherens junctions. The latter is not surprising as endothelial cells are not known to exhibit desmosomes (maculae adherens) (Dejana et al., 1995). It is not clear whether the junctions observed by Grierson were zonula adherences, syndesmos, or a heterotypic adhesion complex.

In contrast, both gap and maculae adherens junctions were observed between JCT cells, and contacts between neighboring inner wall cells contained both gap and occluding junctions. While adherens junctions have not been reported between inner wall cells (Grierson et al., 1978; Raviola and Raviola, 1981; Bhatt et al., 1995; Ye et al., 1997), such junctions are required for both occluding junction and gap junctions formation (Dejana et al., 1995). Consistent with this expectation, Heimark et al. (2002) reported that inner wall cell contain abundant VE-cadherin.

The outer wall of Schlemm's canal, which is not significantly involved in filtration and rests on a more continuous basement membrane, demonstrated no observable contacts with subendothelial fibroblasts, and contacts along the lateral borders between outer wall cells reveals fewer junctional modifications compared to their inner wall counterparts (Grierson et al., 1978). This indicates that the mechanical and hydrodynamic environment of the inner wall may have a functional role in the maintenance and adaptation of intercellular adhesions involved in tethering.

#### 4.1.2. Cell–ECM tethers

An alternative mechanism to secure inner wall cells to their substratum in the face of pressure differentials may involve tethering to the elastic fibers found in the JCT that originate in the ciliary muscle and extend out from the cribriform plexus. Connecting fibrils reach from the cribriform plexus into the JCT where they contact plaque material, basement membrane components or inner wall cells (Rohen et al., 1981; Gong et al., 1996). Rohen observed that cell membranes of inner wall cells were “densified”

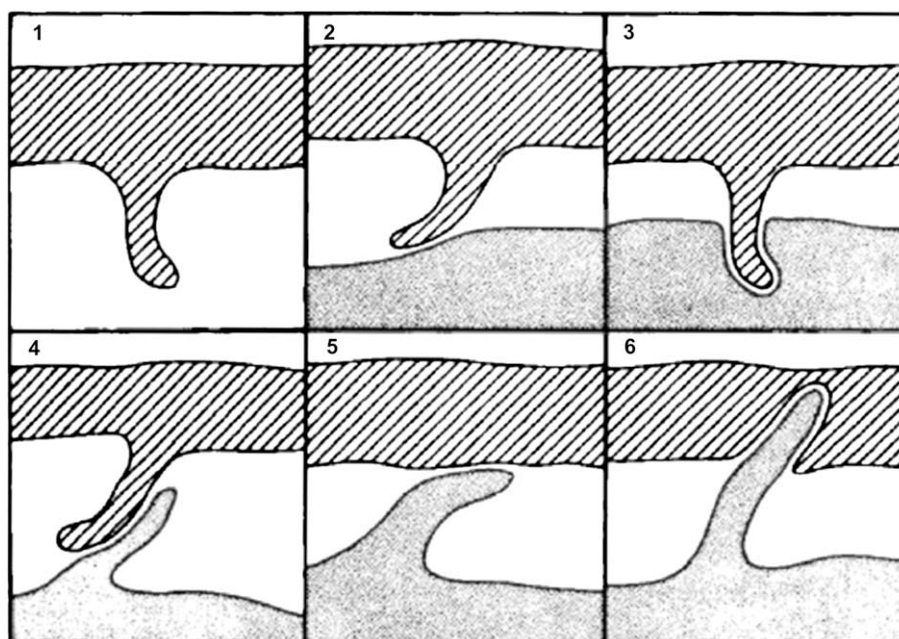


**Fig. 11.** Schematic of contacts between inner wall cells and JCT cells. Crosshatched cells are inner wall cells while shaded cells are JCT cells. Process-to-process contacts (type 4) were most common (~40%) followed by process-to-cell associations (type 5 ~30%; type 2 ~25%). Percentages represent measurements from 1000 regions of contact in 9 rhesus monkey eyes fixed at 15 mm Hg. Adapted with permission from (Grierson et al., 1978).

where the elastic fibrils made contact, resembling adhesion plaques (Rohen et al., 1981). Interestingly, the intracellular filaments of inner wall cells often were in the same orientation as the connecting fibrils, suggesting that these cell–ECM interactions are mechanically continuous and may support mechanical stress (Rohen et al., 1981). The manner by which Schlemm's canal cells attach to elastic fibers is unknown, but is likely via integrin binding to components of elastic “sheath material” that may contain fibrillin-5, fibrillin-1, fibrillin-2 and/or elastin (Rodgers and Weiss, 2005).

Also providing mechanical support for inner wall cells are adhesive interactions with their basement membrane; a discontinuous platform composed mostly of collagen I, IV, fibronectin, laminin 111, 211 (Dietlein et al., 1998) and 511, but not 332 (Stamer, unpublished), heparin sulfate proteoglycans, and to a lesser extent collagens III, V and VI (Rodrigues et al., 1980; Murphy et al., 1987; Tawara et al., 1989; Marshall et al., 1990; Gong et al., 1992; Brilakis et al., 2001; Hann et al., 2001). Cell–ECM adhesions involving integrins and/or syndecans that span the cell membrane and bind to the cytoskeleton are likely involved in tethering the inner wall endothelium to the basement membrane or underlying ECM.

Only two studies have specifically examined integrin subunit expression by inner wall cells. Tervo observed that the two major integrin pairs expressed by Schlemm's canal cells were  $\alpha_5\beta_1$  and  $\alpha_6\beta_1$ , binding fibronectin and laminin, respectively (Tervo et al., 1995), while Zhou confirmed  $\beta_1$  expression in the inner wall and also showed expression of  $\alpha_v\beta_3$ , particularly in young eyes (Zhou et al., 1999). Syndecan-4 is prevalent in the human outflow pathway along with moderate expression of syndecan-3, but very little expression of syndecan-1 and -2 (Filla et al., 2004). Syndecans bind to several ECM ligands, including fibronectin, vitronectin, and many collagens (Alexopoulou et al., 2007). Perfusion with a recombinant HepII domain of fibronectin, that includes both integrin and syndecan binding sites, decreases outflow resistance in human organ culture eyes, with separation of cell linkages to the cribriform plexus as seen using electron microscopy (Santas et al., 2003). As a potential mechanism to increase adhesion, Schlemm's canal cells extend finger-like processes that interdigitate into the basement membrane (Gong et al., 1996), anchoring the cell into the basement membrane and increasing the surface area for integrin or syndecan adhesion.

It is clear that there is a substantial level of attachment between inner wall cells and its underlying substrata. The question then arises as to the strength of these attachments and whether they are strong enough to support the pressure gradient acting on these cells.

#### 4.1.3. Strength of cell–cell and cell–ECM adhesions

To maintain the morphology and function of the outflow pathway, cell–cell and/or cell–ECM adhesions must be physically capable of supporting the loads arising from the pressure drop across these tissues.

The forces necessary to detach adherent cells from fibronectin-coated substrates typically range from 1 to 10 nN/cell, as measured using in vitro centrifugation assays (Lotz et al., 1989; Ward and Hammer, 1993) and micropipette peeling assays of muscle cells seeded on collagen (Ra et al., 1999), while shear stress assays for cell–fibronectin detachment have produced larger estimates of cell adhesion strength of  $\sim 200$  nN (Gallant et al., 2005). Cell detachment has been proposed to occur through a “peeling” mechanism where the detachment front advances through progressive rupture of individual adhesive bonds once the detachment force exceeds the strength of individual bonds at the cell periphery (Dembo et al., 1988; Ward and Hammer, 1993). “Peeling” contrasts with the “fracture” mechanism where many bonds contribute equally to the adhesion force, which would lead to predictions of detachment

forces that are several orders of magnitude larger than those predicted from peeling (Ward and Hammer, 1993).

Using the highest reported cellular adhesion strength of 200 nN (Gallant et al., 2005), we can estimate the maximum pressure loading that inner wall cell attachments could support. Using a cellular surface area for Schlemm's canal cells of approximately  $450 \mu\text{m}^2$  (Lütjen-Drecoll and Rohen, 1970; Bill and Svedbergh, 1972), the maximum pressure loading that could be supported would be approximately 3 mm Hg. As inner wall cell continuity is preserved despite intraocular pressures of 30 mm Hg or higher (Johnstone and Grant, 1973), several possibilities are suggested: (i) the adhesions attaching inner wall cells to their substratum in vivo are much stronger than those measured for other cell types in vitro, (ii) cell–cell attachments are responsible for supporting much of this load or (iii) only a small fraction of the total pressure drop in the aqueous outflow pathway occurs directly across the inner wall endothelium. This latter explanation is consistent with the funneling theory (Johnson et al., 1992) that predicts that, despite the inner wall pores acting to modulate resistance, the bulk of outflow resistance is generated within the JCT.

Mechanical force transmission between cells is typically mediated through cell–cell adhesions involving cadherins (Dejana et al., 1995). While the strength of these adhesions is not as well characterized as for cell–ECM adhesions, it has been suggested that the strength of cadherin adhesions is similar to that of focal adhesions (Chu et al., 2004 (Ganz et al., 2006)). If this is true for adhesions between inner wall cells and JCT cells, then this would indicate that cadherin adhesions would also be mechanically challenged in their ability to support a significant pressure drop across the inner wall endothelium. It is unknown, however, how cell adhesion strength is affected by cell overlap and dynamic junctional remodeling.

Recent data suggest that the inner wall cells themselves may also have difficulty supporting a substantial pressure drop across this endothelium (Ethier et al., 2008). That study concluded that without substantial attachments to the substratum (or to neighboring cells), based on the measured modulus of SC cells (Zeng et al., 2007; Zeng et al., 2008), many cells would fail at pressure drops greater than 2.8 mm Hg. In light of the above considerations, it does not appear that attachments either to the substratum or to neighboring cells would provide sufficient support to these cells. These arguments support the funneling theory, or at least, that the bulk of aqueous outflow resistance is not generated by the inner wall endothelium.

#### 4.2. Biological implications of tethering between the inner wall and JCT

Mechanical forces affect the behavior of living cells by influencing intracellular biochemistry, signaling, gene expression, cytoskeletal contractility and migration (Ingber, 2003). Trabecular meshwork cells have been reported to sense and respond to mechanical stretch by rearranging their cytoskeleton and altering intracellular signaling (tyrosine and MAPK phosphorylation) (Tumminia et al., 1998), and mechanical force applied to trabecular meshwork cells induces up- and down-regulation or alternative splicing of several genes coding for extracellular matrix proteins (Vittal et al., 2005; Keller et al., 2007), including matrix metalloproteinases (Bradley et al., 2001) that act to decrease outflow resistance (Bradley et al., 1998). Such mechanosensitive responses are similar to those observed in many other cells types in the body, including vascular endothelial cells, where integrin-containing focal complexes undergo maturation and directional assembly in response to force (Rivelino et al., 2001) and strengthening of integrin–cytoskeletal linkages occurs when forces are applied to integrins (Choquet et al., 1997; Matthews et al., 2006).

Mechanical stretch, driven by pressure gradients across the outflow pathway, may therefore influence the structure and function of outflow pathway cells and tissues, potentially leading to “feedback” mechanisms that influence outflow resistance. For example, maintaining elevated IOP in a human organ culture model leads over time to a decreased outflow resistance (Borras et al., 2002).

We propose several scenarios by which such feedback might occur. First, the adhesions between the inner wall endothelial cells and their substratum means that any pressure-induced strains will be sensed throughout the trabecular meshwork and JCT, as is known from morphological studies (Johnstone and Grant, 1973). This stretch may influence the cellular expression of genes by any of these cells, such as those involved in ECM biosynthesis or degradation (Bradley et al., 2001) that may contribute to outflow resistance regulation. Borras et al. (2002) showed that increased IOP in the human organ culture model caused an early increase in stromelysin expression that may have contributed to the decrease in outflow resistance observed in that study. However, the dynamic change in gene expression following the change in IOP is likely complicated by the involvement of many protein products.

Second, mechanical stretch acting on JCT or inner wall cells may modulate cellular stiffness or the strength of cell–cell or cell–matrix adhesions, as occurs following integrin clustering or focal adhesion assembly (Choquet et al., 1997; Matthews et al., 2006). These stiffness changes may in turn influence the resistance generating ability of the JCT and inner wall, for example, by affecting the strength of connections between the inner wall and JCT or by influencing the formation of pores or giant vacuoles.

Finally, as mentioned above, the tethering between the inner wall endothelium and its substratum allows the pressure loading to be transmitted to the JCT and trabecular meshwork. The coordinated expansion of outflow tissues with increasing IOP leads to narrowing of Schlemm's canal (Fig. 6), that increases shear stress forces in the canal (Ethier et al., 2004). Shear stress induces many adaptive changes in vascular endothelia (Davies, 1995), and similar shear-responsive mechanisms may allow inner wall cells to sense and respond to changes in IOP. The specific mechanisms by which inner wall cells respond to shear, however, have not been established.

## 5. Future directions

Mechanical and biological interactions between adjacent tissues are common and well-known in vascular systems (Davies et al., 1997). In this review, we have described hydrodynamic, mechanical and biological interactions between the endothelium of Schlemm's canal and the tissues that underlie this endothelium, and we related these findings to the generation of outflow resistance. However, there are a number of areas where further research is needed, and here we give our recommendations for future work.

The funneling model has emerged as an important synergistic mechanism to explain the paradox of outflow resistance generation. However, a number of extensions to the funneling model should be considered. First, funneling introduces “choke points” where local matrix accumulation or subtle changes in cell morphology may have an amplified resistance effect. Thus, a better characterization of the distribution and turnover of macromolecules in the immediate vicinity of pores, giant vacuole basal openings and discontinuities in basement membranes may be of importance. Also, better understanding of regional variations in funneling may improve our knowledge of segmental outflow and how segmental outflow relates to outflow resistance generation.

Along with this, a better characterization of basement membrane discontinuities is long overdue. Do these discontinuities occur in the same locations as giant vacuoles and pores? Does the

formation of one of these structures initiate the formation of the others? One can imagine, for example, that giant vacuole formation leads to a thinning of the endothelial cell that initiates pore formation. The resulting stresses and redistribution of hydrodynamic loads may then lead to focalized ruptures in the basement membrane.

Other important areas of future study include a more detailed characterization of the biomechanics of inner wall cells and their attachment to their substratum and neighboring cells. It is likely that mechanical loads acting on these cells are ultimately transferred to elastic fibers in the JCT (the cribriform plexus) that are extensions of the ciliary muscle (Rohen et al., 1981). The anatomy of these connections has been characterized, but further molecular and biomechanical characterization of these adhesions is needed. What is the strength and level of force that these adhesions can support, and how is adhesion strength affected by inner wall cell processes that interdigitate into the basement membrane? What adhesion molecules are involved, and do these molecules couple to the cytoskeleton? This is particularly important to clarify the mechanism by which accommodation acts to alter outflow resistance (Kaufman and Bány, 1981), which may be important as the ciliary muscle loses its ability to contract with age and may contribute to the pathogenesis of glaucoma (Kaufman and Gabelt, 1995).

A better understanding of transport through the inner wall endothelium must include a characterization of the process of giant vacuole formation in these cells. It is puzzling that more is not known about the dynamic formation of these structures, given that they were discovered a half century ago (Garron et al., 1958). Similar considerations apply to the process of pore formation. Two types of pore have been identified (Ethier et al., 1998); but do they have a common origin, and do they respond differently to changes in IOP? What is the “true” in vivo pore density, and what molecular machinery mediates pore formation? What is the lifetime of a pore? Better in vitro models of pore and giant vacuole formation, perhaps coupled with real-time microscopy, would help answer these questions.

Studies have indicated that the “washout” effect that occurs in animal eyes is associated with a loss of adhesion between the inner wall and JCT (Overby et al., 2002), but which specific adhesion molecules are involved? And why does washout not occur in human eyes? (see Gong et al. in this issue for a review of this subject). A better understanding of the washout mechanism may lead to novel treatments for elevated IOP characteristic of glaucoma.

Finally, the considerations raised here suggest that while the inner wall endothelium might modulate outflow resistance, the bulk of outflow resistance generation likely lies within the JCT and/or basement membrane of the inner wall endothelium. Determining which specific ECM molecules might be involved in outflow resistance generation will require more advanced imaging techniques, perhaps requiring environmental scanning electron microscopy (Fautsch and Johnson, 2006). Such studies will likely require biochemical characterization and stereological analysis (Overby and Johnson, 2005) to relate resistance generation to specific ultrastructure features within the JCT.

## Acknowledgements

We gratefully acknowledge the lasting contributions of Doug Johnson who inspired, nurtured, and challenged our ideas on outflow resistance generation. We acknowledge support from NIH grants EY018373 (DRO), EY09699 (MJ), EY17007 (WDS), National Glaucoma Research, a program American Health Assistance Foundation, NGR-G2006-057 (DRO), and Research to Prevent Blindness Foundation (WDS).

## References

- Acott, T.S., Kingsley, P.D., Samples, J.R., Van Buskirk, E.M., 1988. Human trabecular meshwork organ culture: morphology and glycosaminoglycan synthesis. *Investig. Ophthalmol. Vis. Sci.* 29, 90–100.
- Alexopoulou, A.N., Multhaupt, H.A., Couchman, J.R., 2007. Syndecans in wound healing, inflammation and vascular biology. *Int. J. Biochem. Cell Biol.* 39, 505–528.
- Allingham, R.R., de Kater, A.W., Ethier, C.R., Anderson, P.J., Hertzmark, E., Epstein, D.L., 1992. The relationship between pore density and outflow facility in human eyes. *Investig. Ophthalmol. Vis. Sci.* 33, 1661–1669.
- Alvarado, J.A., Yun, A.J., Murphy, C.G., 1986. Juxtacanalicular tissue in primary open angle glaucoma and in nonglaucomatous normals. *Arch. Ophthalmol.* 104, 1517–1528.
- Bahler, C.K., Hann, C.R., Fautsch, M.P., Johnson, D.H., 2004. Pharmacologic disruption of Schlemm's canal cells and outflow facility in anterior segments of human eyes. *Investig. Ophthalmol. Vis. Sci.* 45, 2246–2254.
- Bárány, E.H., 1953. In vitro studies of the resistance to flow through the angle of the anterior chamber. *Acta Soc. Med. Ups.* 59, 260–276.
- Bárány, E.H., Scotchbrook, S., 1954. Influence of testicular hyaluronidase on the resistance to flow through the angle of the anterior chamber. *Acta Physiol. Scand.* 30, 240–248.
- Bárány, E.H., Woodin, A.M., 1955. Hyaluronic acid and hyaluronidase in the aqueous humor and the angle of the anterior chamber. *Acta Physiol. Scand.* 33, 257–290.
- Battista, S.A., Lu, Z., Hofmann, S., Freddo, T.F., Overby, D., Gong, H., 2008. Acute IOP elevation reduces the available area for aqueous humor outflow and induces meshwork herniations into collector channels of bovine eyes. *Investig. Ophthalmol. Vis. Sci.* 49, 5346–5352.
- Bhatt, K., Gong, H., Freddo, T.F., 1995. Freeze-fracture studies of interendothelial junctions in the angle of the human eye. *Investig. Ophthalmol. Vis. Sci.* 36, 1379–1389.
- Bill, A., 1970. Scanning electron microscopic studies of the canal of Schlemm. *Exp. Eye Res.* 10, 214.
- Bill, A., 1975. Blood circulation and fluid dynamics in the eye. *Physiol. Rev.* 55, 383–416.
- Bill, A., Lütjen-Drecoll, E., Svedbergh, B., 1980. Effects of intracameral  $\text{NA}_2\text{EDTA}$  and EGTA on aqueous outflow routes in the monkey eye. *Investig. Ophthalmol. Vis. Sci.* 19, 492–504.
- Bill, A., Svedbergh, B., 1972. Scanning electron microscopic studies of the trabecular meshwork and the canal of Schlemm – an attempt to localize the main resistance to outflow of aqueous humor in man. *Acta Ophthalmol.* 50, 295–320.
- Borras, T., Rowlette, L.L., Tamm, E.R., Gottanka, J., Epstein, D.L., 2002. Effects of elevated intraocular pressure on outflow facility and TIGR/MYOX expression in perfused human anterior segments. *Investig. Ophthalmol. Vis. Sci.* 43, 33–40.
- Bos, K.J., Holmes, D.F., Meadows, R.S., Kadler, K.E., McLeod, D., Bishop, P.N., 2001. Collagen fibril organisation in mammalian vitreous by freeze etch/rotary shadowing electron microscopy. *Micron* 32, 301–306.
- Bradley, J.M., Vranka, J., Colvis, C.M., Conger, D.M., Alexander, J.P., Fisk, A.S., Samples, J.R., Acott, T.S., 1998. Effect of matrix metalloproteinases activity on outflow in perfused human organ culture. *Investig. Ophthalmol. Vis. Sci.* 39, 2649–2658.
- Bradley, J.M.B., Kelley, M.J., Zhu, X., Anderssohn, A.M., Alexander, J.P., Acott, T.S., 2001. Effects of mechanical stretching on trabecular matrix metalloproteinases. *Investig. Ophthalmol. Vis. Sci.* 42, 1505–1513.
- Briaklis, H.S., Hann, C.R., Johnson, D.H., 2001. A comparison of different embedding media on the ultrastructure of the trabecular meshwork. *Curr. Eye Res.* 22, 235–244.
- Briaklis, H.S., Johnson, D.H., 2001. Giant vacuole survival time and implications for aqueous humor outflow. *J. Glaucoma.* 10, 277–283.
- Brubaker, R.F., 1975. The effect of intraocular pressure on conventional outflow resistance in the enucleated human eye. *Investig. Ophthalmol. Vis. Sci.* 14, 286–292.
- Buller, C., Johnson, D., 1994. Segmental variability of the trabecular meshwork in normal and glaucomatous eyes. *Investig. Ophthalmol. Vis. Sci.* 35, 3841–3851.
- Choquet, D., Felsenfeld, D.P., Sheetz, M.P., 1997. Extracellular matrix rigidity causes strengthening of integrin-cytoskeleton linkages. *Cell* 88, 39–48.
- Chu, Y.S., Thomas, W.A., Eder, O., Pincet, F., Perez, E., Thiery, J.P., Dufour, S., 2004. Force measurements in e-cadherin-mediated cell doublets reveal rapid adhesion strengthened by actin cytoskeleton remodeling through rac and cdc42. *J. Cell Biol.* 167, 1183–1194.
- Collaborative Normal-Tension Glaucoma Study Group, 1998. Comparison of glaucomatous progression between untreated patients with normal-tension glaucoma and patients with therapeutically reduced intraocular pressures. *Am. J. Ophthalmol.* 126, 487–497.
- Davies, P.F., 1995. Flow-mediated endothelial mechanotransduction. *Physiol. Rev.* 75, 519–560.
- Davies, P.F., Barbee, K.A., Volin, M.V., Robotewskyj, A., Chen, J., Joseph, L., Griem, M.L., Wernick, M.N., Jacobs, E., Polacek, D.C., dePaola, N., Barakat, A.I., 1997. Spatial relationships in early signaling events of flow-mediated endothelial mechanotransduction. *Annu. Rev. Physiol.* 59, 527–549.
- Dejana, E., Corada, M., Lampugnani, M.G., 1995. Endothelial cell-to-cell junctions. *FASEB J.* 9, 910–918.
- Dembo, M., Torney, D.C., Saxman, K., Hammer, D., 1988. The reaction-limited kinetics of membrane-to-surface adhesion and detachment. *Proc. R. Soc. Lond. B Biol. Sci.* 234, 55–83.
- Dietlein, T.S., Jacobi, P.C., Paulsson, M., Smyth, N., Kriegelstein, G.K., 1998. Laminin heterogeneity around Schlemm's canal in normal humans and glaucoma patients. *Ophthalmic Res.* 30, 380–387.
- Dvorak-Theobald, G., 1934. Schlemm's canal: its anastomoses and anatomic relations. *Trans. Am. Ophthalmol. Soc.* 32, 574–595.
- Ellingsen, B.A., Grant, W.M., 1972. Trabeculotomy and sinusotomy in enucleated human eyes. *Investig. Ophthalmol.* 11, 21–28.
- Erickson-Lamy, K., Schroeder, A.M., Bassett-Chu, S., Epstein, D.L., 1990. Absence of time-dependent facility increase (“Washout”) in the perfused enucleated human eye. *Investig. Ophthalmol. Vis. Sci.* 31, 2384–2388.
- Eriksson, A., Svedbergh, B., 1980. Transcellular aqueous humor outflow: A theoretical and experimental study. *Albrecht Von Graefes Arch. Klin. Exp. Ophthalmol.* 212, 187–197.
- Ethier, C.R., Chan, D.W., 2001. Cationic ferritin changes outflow facility in human eyes whereas anionic ferritin does not. *Investig. Ophthalmol. Vis. Sci.* 42, 1795–1802.
- Ethier, C.R., Coloma, F.M., 1999. Effects of ethacrynic acid on Schlemm's canal inner wall and outflow facility in human eyes. *Investig. Ophthalmol. Vis. Sci.* 40, 1599–1607.
- Ethier, C.R., Coloma, F.M., Sit, A.J., Johnson, M., 1998. Two pore types in the inner wall endothelium of Schlemm's canal. *Investig. Ophthalmol. Vis. Sci.* 39, 2041–2048.
- Ethier, C.R., Croft, M.A., Coloma, F.M., Gangnon, R.E., Ladd, W., Kaufman, P.L., 1999. Ethacrynic acid effects on inner wall pores in living monkeys. *Investig. Ophthalmol. Vis. Sci.* 40, 1382–1391.
- Ethier, C.R., Kamm, R.D., Palaszewski, B.A., Johnson, M., Richardson, T.M., 1986. Calculations of flow resistance in the juxtacanalicular meshwork. *Investig. Ophthalmol. Vis. Sci.* 27, 1741–1750.
- Ethier, C.R., Read, A.T., Chan, D., 2004. Biomechanics of Schlemm's canal endothelial cells: influence on f-actin architecture. *Biophys. J.* 87, 2828–2837.
- Ethier, C.R., Read, A.T., Chan, D.W., 2006. Effects of latrunculin-B on outflow facility and trabecular meshwork structure in human eyes. *Investig. Ophthalmol. Vis. Sci.* 47, 1991–1998.
- Ethier, C.R., Zeng, D., Read, A.T., Chan, D.W., Gong, H., Johnson, M., 2008. Pressure-induced deformation of Schlemm's canal endothelial cells [ARVO Abstract #1633]. *Invest. Ophthalmol. Vis. Sci.* 49, 1633.
- Fautsch, M.P., Johnson, D.H., 2006. Aqueous humor outflow: what do we know? Where will it lead us? *Investig. Ophthalmol. Vis. Sci.* 47, 4181–4187.
- Filla, M.S., David, G., Weinreb, R.N., Kaufman, P.L., Peters, D.M., 2004. Distribution of syndecans 1–4 within the anterior segment of the human eye: expression of a variant syndecan-3 and matrix-associated syndecan-2. *Exp. Eye Res.* 79, 61–74.
- Freddo, T.F., 1993. Ocular anatomy and physiology related to aqueous production and outflow. In: Lewis, T.L., Fingeret, M. (Eds.), *Primary Care of the Glaucomas*. Appleton & Lange, Norwalk, pp. 23–46.
- Gallant, N.D., Michael, K.E., Garcia, A.J., 2005. Cell adhesion strengthening: contributions of adhesive area, integrin binding, and focal adhesion assembly. *Mol. Biol. Cell* 16, 4329–4340.
- Garron, L.K., Feeny, M.L., Hogan, M.J., McEwen, W.K., 1958. Electron microscopic studies of the human eye. I. Preliminary investigations of the trabeculas. *Am. J. Ophthalmol.* 46, 27–35.
- Ganz, A., Lambert, M., Saez, A., Silberzan, P., Buguin, A., Mege, R.M., Ladoux, B., 2006. Traction forces exerted through N-cadherin contacts. *Biol. Cell.* 98, 721–730.
- Gong, H., Freddo, T.F., Johnson, M., 1992. Age-related changes of sulfated proteoglycans in the normal human trabecular meshwork. *Exp. Eye Res.* 55, 691–709.
- Gong, H., Ruberti, J., Overby, D., Johnson, M., Freddo, T., 2002. A new view of the human trabecular meshwork using quick-freeze, deep-etch electron microscopy. *Exp. Eye Res.* 75, 347–358.
- Gong, H., Tripathi, R.C., Tripathi, B.J., 1996. Morphology of the aqueous outflow pathway. *Microsc. Res. Tech.* 33, 336–367.
- Gottanka, J., Johnson, D.H., Martus, P., Lütjen-Drecoll, E., 2001. Beta-adrenergic blocker therapy and the trabecular meshwork. *Graefes Arch. Clin. Exp. Ophthalmol.* 239, 138–144.
- Grant, W.M., 1958. Further studies on facility of flow through the trabecular meshwork. *Arch. Ophthalmol.* 60, 523.
- Grant, W.M., 1963. Experimental aqueous perfusion in enucleated human eyes. *Arch. Ophthalmol.* 69, 783–801.
- Grierson, I., Lee, W.R., 1974. Changes in the monkey outflow apparatus at graded levels of intraocular pressure: a qualitative analysis by light microscopy and scanning electron microscopy. *Exp. Eye Res.* 19, 21–33.
- Grierson, I., Lee, W.R., 1975a. Pressure-induced changes in the ultrastructure of the endothelium lining Schlemm's canal. *Am. J. Ophthalmol.* 80, 863–884.
- Grierson, I., Lee, W.R., 1975b. The fine structure of the trabecular meshwork at graded levels of intraocular pressure. (1) Pressure effects within the near-physiological range (8–30 mm Hg). *Exp. Eye Res.* 20, 505–521.
- Grierson, I., Lee, W.R., 1975c. The fine structure of the trabecular meshwork at graded levels of intraocular pressure. (2) Pressures outside the physiological range (0 and 50 mm Hg). *Exp. Eye Res.* 20, 523–530.
- Grierson, I., Lee, W.R., 1977. Light microscopic quantitation of the endothelial vacuoles in Schlemm's canal. *Am. J. Ophthalmol.* 84, 234–246.
- Grierson, I., Lee, W.R., 1978. Pressure effects on flow channels in the lining endothelium of Schlemm's canal: a quantitative study by transmission electron microscopy. *Acta Ophthalmol.* 56, 935–952.
- Grierson, I., Lee, W.R., Abraham, S., Howes, R.C., 1978. Associations between the cells of the walls of Schlemm's canal. *Albrecht Von Graefes Arch. Klin. Exp. Ophthalmol.* 208, 33–47.

- Grierson, I., Lee, W.R., Moseley, H., Abraham, S., 1979. The trabecular wall of Schlemm's canal: a study of the effects of pilocarpine by scanning electron microscopy. *Br. J. Ophthalmol.* 63, 9–16.
- Hamanaka, T., Bill, A., 1987. Morphological and functional effects of  $\text{Na}_2\text{EDTA}$  on the outflow routes for aqueous humor in monkeys. *Exp. Eye Res.* 44, 171–190.
- Hamanaka, T., Bill, A., 1988. Effects of alpha-chymotrypsin on the outflow routes for aqueous humor. *Exp. Eye Res.* 46, 323–341.
- Hann, C.R., Bahler, C.K., Johnson, D.H., 2005. Cationic ferritin and segmental flow through the trabecular meshwork. *Investig. Ophthalmol. Vis. Sci.* 46, 1–7.
- Hann, C.R., Springett, M.J., Johnson, D.H., 2001. Antigen retrieval of basement membrane proteins from archival eye tissues. *J. Histochem. Cytochem.* 49, 475–482.
- Happel, J., Brenner, H., 1983. *Low Reynolds Number Hydrodynamics*. Martinus Nijhoff, The Hague.
- Hascall, V.C., Hascall, G.K., 1982. Proteoglycans. In: Hay, E.D. (Ed.), *Cell Biology of Extracellular Matrix*. Plenum, New York, pp. 39–63.
- Heimark, R.L., Kaochar, S., Stamer, W.D., 2002. Human Schlemm's canal cells express the endothelial adherens proteins, VE-cadherin and PECAM-1. *Curr. Eye Res.* 25, 299–308.
- Hoffman, F., Dumitrescu, L., 1971. Schlemm's canal under the scanning electron microscope. *Ophthalmic Res.* 2, 37–45.
- Holmberg, A., 1959. The fine structure of the inner wall of Schlemm's canal. *Arch. Ophthalmol.* 62, 956–958.
- Hubbard, W.C., Johnson, M., Gong, H., Gabelt, B.T., Petersen, J.A., Sawhney, R., Freddo, T.F., Kaufman, P.L., 1997. Intraocular pressure and outflow facility are unchanged following acute and chronic intracameral chondroitinase ABC and hyaluronidase in monkeys. *Exp. Eye Res.* 65, 177–190.
- Ingber, D.E., 2003. Mechanobiology and diseases of mechanotransduction. *Ann. Med.* 35, 564–577.
- Inomata, H., Bill, A., Smelser, G.K., 1972. Aqueous humor pathways through the trabecular meshwork and into Schlemm's canal in cynomolgus monkey (*macaca irus*). *Am. J. Ophthalmol.* 73, 760–789.
- Ishizaki, T., Uehata, M., Tamechika, I., Keel, J., Nonomura, K., Maekawa, M., Narumiya, S., 2000. Pharmacological properties of Y-27632, a specific inhibitor of RHO-associated kinases. *Mol. Pharmacol.* 57, 976–983.
- Johnson, D.H., 1997. The effect of cytochalasin D on outflow facility and the trabecular meshwork of the human eye in perfusion organ culture. *Investig. Ophthalmol. Vis. Sci.* 38, 2790–2799.
- Johnson, M., 2006. What controls aqueous humour outflow resistance? *Exp. Eye Res.* 82, 545–557.
- Johnson, M., Chan, D., Read, A.T., Christensen, C., Sit, A., Ethier, C.R., 2002. The pore density in the inner wall endothelium of Schlemm's canal of glaucomatous eyes. *Investig. Ophthalmol. Vis. Sci.* 43, 2950–2955.
- Johnson, M., Erickson, K., 2000. Mechanisms and routes of aqueous humor drainage. In: Albert, D.M., Jakobiec, F.A. (Eds.), *Principles and Practice of Ophthalmology*, vol. 4. WB Saunders Co., Philadelphia, pp. 2577–2595 (Chapter 193B, Glaucoma).
- Johnson, M., Gong, H., Freddo, T.F., Ritter, N., Kamm, R., 1993. Serum proteins and aqueous outflow resistance in bovine eyes. *Investig. Ophthalmol. Vis. Sci.* 34, 3549–3557.
- Johnson, M., Kamm, R.D., 1983. The role of Schlemm's canal in aqueous outflow from the human eye. *Investig. Ophthalmol. Vis. Sci.* 24, 320–325.
- Johnson, M., Shapiro, A., Ethier, C.R., Kamm, R.D., 1992. Modulation of outflow resistance by the pores of the inner wall endothelium. *Investig. Ophthalmol. Vis. Sci.* 33, 1670–1675.
- Johnstone, M.A., 1979. Pressure-dependent changes in nuclei and the process origins of the endothelial cells lining Schlemm's canal. *Investig. Ophthalmol. Vis. Sci.* 18, 44–51.
- Johnstone, M.A., Grant, W.G., 1973. Pressure-dependent changes in structures of the aqueous outflow system of human and monkey eyes. *Am. J. Ophthalmol.* 75, 365–383.
- de Kater, A.W., Melamed, S., Epstein, D.L., 1989. Patterns of aqueous humor outflow in glaucomatous and nonglaucomatous human eyes: a tracer study using cationized ferritin. *Arch. Ophthalmol.* 107, 572–576.
- Kass, M.A., Heuer, D.K., Higginbotham, E.J., Johnson, C.A., Keltner, J.L., Miller, J.P., Parrish 2nd, R.K., Wilson, M.R., Gordon, M.O., 2002. The ocular hypertension treatment study: a randomized trial determines that topical ocular hypotensive medication delays or prevents the onset of primary open-angle glaucoma. *Arch. Ophthalmol.* 120, 701–713.
- Kaufman, P.L., Bärány, E.H., 1981. Adrenergic drug effects on aqueous outflow facility following ciliary muscle retrodisplacement in the cynomolgus monkey. *Investig. Ophthalmol. Vis. Sci.* 20, 644.
- Kaufman, P.L., Gabelt, B.T., 1995. Presbyopia, prostaglandins and primary open angle glaucoma. In: Krieglstein, G.K. (Ed.), *Glaucoma Update V: Proceedings of the Symposium of the Glaucoma Society of the International Congress of Ophthalmology in Quebec City, June 1994*. Springer-Verlag, New York-Berlin, pp. 224–241.
- Kayes, J., 1967. Pore structure of the inner wall of Schlemm's canal. *Investig. Ophthalmol. Vis. Sci.* 6, 381–394.
- Keller, K.E., Bradley, J.M., Kelley, M.J., Acott, T.S., 2008. Effects of modifiers of glycosaminoglycan biosynthesis on outflow facility in perfusion culture. *Investig. Ophthalmol. Vis. Sci.* 49, 2495–2505.
- Keller, K.E., Kelley, M.J., Acott, T.S., 2007. Extracellular matrix gene alternative splicing by trabecular meshwork cells in response to mechanical stretching. *Investig. Ophthalmol. Vis. Sci.* 48, 1164–1172.
- Kiland, J.A., Gabelt, B.T., Kaufman, P.L., 2005. Effect of age on outflow resistance washout during anterior chamber perfusion in rhesus and cynomolgus monkeys. *Exp. Eye Res.*
- Knepper, P.A., Farbman, A.I., Telser, A.G., 1984. Exogenous hyaluronidases and degradation of hyaluronic acid in the rabbit eye. *Investig. Ophthalmol. Vis. Sci.* 25, 286–293.
- Knepper, P.A., Goossens, W., Hvizd, M., Palmberg, P.F., 1996a. Glycosaminoglycans of the human trabecular meshwork in primary open-angle glaucoma. *Investig. Ophthalmol. Vis. Sci.* 37, 1360–1367.
- Knepper, P.A., Goossens, W., Palmberg, P.F., 1996b. Glycosaminoglycan stratification of the juxtacanalicular tissue in normal and primary open-angle glaucoma. *Investig. Ophthalmol. Vis. Sci.* 37, 2414–2425.
- Leber, T., 1873. Studien über den flüssigkeitswechsel im auge. *Albrecht Von Graefes Arch. Ophthalmol.* 19, 87–106.
- Lee, W.R., Grierson, I., 1975. Pressure effects on the endothelium of the trabecular wall of Schlemm's canal: a study by scanning electron microscopy. *Albrecht Von Graefes Arch. Klin. Exp. Ophthalmol.* 196, 255–265.
- Levick, J.R., 1987. Flow through interstitium and other fibrous matrices. *Q. J. Exp. Physiol.* 72, 409–437.
- Lotz, M.M., Burdsal, C.A., Erickson, H.P., McClay, D.R., 1989. Cell adhesion to fibronectin and tenascin: quantitative measurements of initial binding and subsequent strengthening response. *J. Cell Biol.* 109, 1795–1805.
- Lu, Z., Overby, D.R., Scott, P.A., Freddo, T.F., Gong, H., 2008. The mechanism of increasing outflow facility by RHO-kinase inhibition with Y-27632 in bovine eyes. *Exp. Eye Res.* 86, 271–281.
- Lütjen-Drecoll, E., Rohen, J.W., 1970. Endothelial studies of the Schlemm's canal using silver-impregnation technique. *Albrecht Von Graefes Arch. Klin. Exp. Ophthalmol.* 180, 249–266.
- Lütjen-Drecoll, E., Shimizu, T., Rohrbach, M., Rohen, J.W., 1986. Quantitative analysis of 'plaque material' between ciliary muscle tips in normal- and glaucomatous eyes. *Exp. Eye Res.* 42, 457–465.
- MacRae, D., Sears, M.L., 1970. Peroxidase passage through the outflow channels of human and rhesus eyes. *Exp. Eye Res.* 10, 15–18.
- Mäepea, O., Bill, A., 1989. The pressures in the episcleral veins, Schlemm's canal and the trabecular meshwork in monkeys: effects of changes in intraocular pressure. *Exp. Eye Res.* 49, 645–663.
- Mäepea, O., Bill, A., 1992. Pressures in the juxtacanalicular tissue and Schlemm's canal in monkeys. *Exp. Eye Res.* 54, 879–883.
- Maniotis, A.J., Chen, C.S., Ingber, D.E., 1997. Demonstration of mechanical connections between integrins, cytoskeletal filaments, and nucleoplasm that stabilize nuclear structure. *Proc. Natl. Acad. Sci. U. S. A.* 94, 849–854.
- Marshall, G.E., Konstas, A.G., Lee, W.R., 1990. Immunogold localization of type IV collagen and laminin in the aging human outflow system. *Exp. Eye Res.* 51, 691–699.
- Matthews, B.D., Overby, D.R., Mannix, R., Ingber, D.E., 2006. Cellular adaptation to mechanical stress: role of integrins, rho, cytoskeletal tension and mechanosensitive ion channels. *J. Cell Sci.* 119, 508–518.
- McEwen, W.K., 1958. Application of Poiseuille's law to aqueous outflow. *Arch. Ophthalmol.* 60, 290.
- Melton, C.E., DeVille, W.B., 1960. Perfusion studies on eyes of four species. *Am. J. Ophthalmol.* 50, 302–308.
- Minckler, D.S., Baerveldt, G., Alfaro, M.R., Francis, B.A., 2005. Clinical results with the Trabectome for treatment of open-angle glaucoma. *Ophthalmology* 112, 962–967.
- Moseley, H., Grierson, I., Lee, W.R., 1983. Mathematical modelling of aqueous humor outflow from the eye through the pores in the lining of Schlemm's canal. *Clin. Phys. Physiol. Meas.* 4, 47–63.
- Moses, R.A., 1977. The effect of intraocular pressure on resistance to outflow. *Surv. Ophthalmol.* 22, 88–100.
- Moses, R.A., 1979. Circumferential flow in Schlemm's canal. *Am. J. Ophthalmol.* 88, 585–591.
- Murphy, C.G., Johnson, M., Alvarado, J.A., 1992. Juxtacanalicular tissue in pigmentary and primary open angle glaucoma. The hydrodynamic role of pigment and other constituents. *Arch. Ophthalmol.* 110, 1779–1785.
- Murphy, C.G., Yun, A.J., Newsome, D.A., Alvarado, J.A., 1987. Localization of extracellular proteins of the human trabecular meshwork by indirect immunofluorescence. *Am. J. Ophthalmol.* 104, 33–43.
- Nesterov, A.P., 1970. Role of blockade of Schlemm's canal in pathogenesis of primary open angle glaucoma. *Am. J. Ophthalmol.* 70, 691–696.
- Nilsson, S.F., 1997. The uveoscleral outflow routes. *Eye* 11, 149–154.
- Overby, D., Gong, H., Freddo, T., Johnson, M., 2002. The mechanism of increasing outflow facility during washout in the bovine eye. *Investig. Ophthalmol. Vis. Sci.* 43, 3455–3464.
- Overby, D., Johnson, M., 2005. Studies of depth-of-field effects in microscopy supported by numerical simulations. *J. Microsc.* 220, 176–189.
- Overby, D., Hofmann, S., Folz, S., Kasper, S., Lu, Z., Scott, P., Gong, H., 2006. The relationship between the hydrodynamic patterns of aqueous humor outflow and outflow resistance. In: Liepsch, D. (Ed.), *Proceedings from the 5th World Congress of Biomechanics in Munich, Germany*. Medimond, Bologna, Italy.
- Pedler, C., 1956. The relationship of hyaluronidase to aqueous outflow resistance. *Trans. Ophthalmol. Soc. U. K.* 76, 51–63.
- Peterson, W.S., Jocson, V.L., 1974. Hyaluronidase effects on aqueous outflow resistance. *Am. J. Ophthalmol.* 77, 573–577.
- Ra, H.J., Picart, C., Feng, H., Sweeney, H.L., Discher, D.E., 1999. Muscle cell peeling from micropatterned collagen: direct probing of focal and molecular properties of matrix adhesion. *J. Cell Sci.* 112, 1425–1436.
- Raviola, C., Raviola, E., 1981. Paracellular route of aqueous outflow in the trabecular meshwork and canal of Schlemm. A freeze-fracture study of the endothelial

- junctions in the sclerocorneal angle of the macaque monkey eye. *Investig. Ophthalmol. Vis. Sci.* 21, 52–72.
- Riveline, D., Zamir, E., Balaban, N.Q., Schwarz, U.S., Ishizaki, T., Narumiya, S., Kam, Z., Geiger, B., Bershadsky, A.D., 2001. Focal contacts as mechanosensors: externally applied local mechanical force induces growth of focal contacts by an mDia1-dependent and ROCK-independent mechanism. *J. Cell Biol.* 153, 1175–1186.
- Rodgers, U.R., Weiss, A.S., 2005. Cellular interactions with elastin. *Pathol. Biol.* 53, 390–398.
- Rodrigues, M.M., Katz, S.I., Foidart, J.M., Spaeth, G.L., 1980. Collagen, factor viii antigen, and immunoglobulins in the human aqueous drainage channels. *Ophthalmology* 87, 337–345.
- Rohen, J.W., Futa, R., Lütjen-Drecoll, E., 1981. The fine structure of the cribriform meshwork in normal and glaucomatous eyes as seen in tangential sections. *Investig. Ophthalmol. Vis. Sci.* 21, 574–585.
- Rohen, J.W., Rentsch, F.J., 1968. Morphology of Schlemm's canal and related vessels in the human eye. *Albrecht Von Graefes Arch. Klin. Exp. Ophthalmol.* 176, 309–329.
- Rosenquist, R., Epstein, D., Melamed, S., Johnson, M., Grant, W.M., 1989. Outflow resistance of enucleated human eyes at two different perfusion pressures and different extents of trabeculotomy. *Curr. Eye Res.* 8, 1233–1240.
- Sabanay, I., Gabelt, B.T., Tian, B., Kaufman, P.L., Geiger, B., 2000. H-7 effects on the structure and fluid conductance of monkey trabecular meshwork. *Arch. Ophthalmol.* 118, 955–962.
- Sabanay, I., Tian, B., Gabelt, B.T., Geiger, B., Kaufman, P.L., 2004. Functional and structural reversibility of H-7 effects on the conventional aqueous outflow pathway in monkeys. *Exp. Eye Res.* 78, 137–150.
- Santas, A.J., Bahler, C., Peterson, J.A., Filla, M.S., Kaufman, P.L., Tamm, E.R., Johnson, D.H., Peters, D.M., 2003. Effect of heparin II domain of fibronectin on aqueous outflow in cultured anterior segments of human eyes. *Investig. Ophthalmol. Vis. Sci.* 44, 4796–4804.
- Sawaguchi, S., Yue, B.Y., Yeh, P., Tso, M.O., 1992. Effects of intracameral injection of chondroitinase ABC in vivo. *Arch. Ophthalmol.* 110, 110–117.
- Scott, P.A., Overby, D.R., Freddo, T.F., Gong, H., 2007. Comparative studies between species that do and do not exhibit the washout effect. *Exp. Eye Res.* 84, 435–443.
- Segawa, K., 1973. Pore structures of the endothelial cells of the aqueous outflow pathway: scanning electron microscopy. *Jpn. J. Ophthalmol.* 17, 133–139.
- Seiler, T., Wollensak, J., 1985. The resistance of the trabecular meshwork to aqueous humor outflow. *Albrecht Von Graefes Arch. Klin. Exp. Ophthalmol.* 223, 88–91.
- Sit, A.J., Coloma, F.M., Ethier, C.R., Johnson, M., 1997. Factors affecting the pores of the inner wall endothelium of Schlemm's canal. *Investig. Ophthalmol. Vis. Sci.* 38, 1517–1525.
- Speakman, J.S., 1959. Aqueous outflow channels in the trabecular meshwork in man. *Br. J. Ophthalmol.* 43, 129.
- Svedbergh, B., 1976. Effects of intraocular pressure on the pores of the inner wall of Schlemm's canal: A scanning electron microscopic study. *Jpn. J. Ophthalmol.* 20, 127.
- Tawara, A., Varner, H.H., Hollyfield, J.G., 1989. Distribution and characterization of sulfated proteoglycans in the human trabecular tissue. *Investig. Ophthalmol. Vis. Sci.* 30, 2215–2231.
- Ten Hulzen, R.D., Johnson, D.H., 1996. Effect of fixation pressure on juxtacanalicular tissue and Schlemm's canal. *Investig. Ophthalmol. Vis. Sci.* 37, 114–124.
- Tervo, K., Päällysaho, T., Virtanen, I., Tervo, T., 1995. Integrins in human anterior chamber angle. *Graefes Arch. Clin. Exp. Ophthalmol.* 233, 291–292.
- Tian, B., Kaufman, P., Vollberg, T., Gabelt, B., Geiger, B., 1998. H-7 disrupts the actin cytoskeleton and increases outflow facility. *Arch. Ophthalmol.* 116, 633–643.
- Tumminia, S.J., Mitton, K.P., Arora, J., Zelenka, P., Epstein, D.L., Russell, P., 1998. Mechanical stretch alters the actin cytoskeletal network and signal transduction in human trabecular meshwork cells. *Investig. Ophthalmol. Vis. Sci.* 39, 1361–1371.
- Tripathi, R.C., 1974. Comparative physiology and anatomy of the aqueous outflow pathway. In: Davson, H., Graham, J.R., L.T. (Eds.), *The Eye*. Academic Press, New York, pp. 163–356.
- Uehata, M., Ishizaki, T., Satoh, H., Ono, T., Kawahara, T., Morishita, T., Tamakawa, H., Yamagami, K., Inui, J., Maekawa, M., Narumiya, S., 1997. Calcium sensitization of smooth muscle mediated by a RHO-associated protein kinase in hypertension. *Nature* 389, 990–994.
- Van Buskirk, E.M., 1976. Changes in the facility of aqueous outflow induced by lens depression and intraocular pressure in excised human eyes. *Am. J. Ophthalmol.* 82, 736–740.
- Van Buskirk, E.M., 1977. Trabeculotomy in the immature, enucleated human eye. *Investig. Ophthalmol. Vis. Sci.* 16, 63–66.
- Van Buskirk, E.M., Grant, W.M., 1973. Lens depression and aqueous outflow in enucleated primate eyes. *Am. J. Ophthalmol.* 72, 632–640.
- Van Buskirk, M.S., Brett, J., 1978. The canine eye: in vitro dissolution of the barriers to aqueous outflow. *Investig. Ophthalmol. Vis. Sci.* 17, 258–263.
- Vittal, V., Rose, A., Gregory, K.E., Kelley, M.J., Acott, T.S., 2005. Changes in gene expression by trabecular meshwork cells in response to mechanical stretching. *Investig. Ophthalmol. Vis. Sci.* 46, 2857–2868.
- Ward, M.D., Hammer, D.A., 1993. A theoretical analysis for the effect of focal contact formation on cell-substrate attachment strength. *Biophys. J.* 64, 936–959.
- Wise, J.B., Witter, S.L., 1979. Argon laser therapy for open-angle glaucoma. A pilot study. *Arch. Ophthalmol.* 97, 319–322.
- Yan, D.B., Trope, G.E., Ethier, C.R., Menon, I.A., Wakeham, A., 1991. Effects of hydrogen peroxide-induced oxidative damage on outflow facility and washout in pig eyes. *Investig. Ophthalmol. Vis. Sci.* 32, 2515–2520.
- Ye, W., Gong, H., Sit, A., Johnson, M., Freddo, T.F., 1997. Interendothelial junctions in normal human Schlemm's canal respond to changes in pressure. *Investig. Ophthalmol. Vis. Sci.* 38, 2460–2468.
- Zeng, D., Juzkiw, T., Ethier, C.R., Johnson, M., 2007. Estimating Young's modulus of Schlemm's canal endothelial cells [ARVO Abstract #2074]. *Invest. Ophthalmol. Vis. Sci.* 48, 2074.
- Zeng, D., Juzkiw, T., Read, A.T., Chan, D.W.-H., Glucksberg, M.R., Ethier, C.R., Johnson, M., 2008. Young's modulus of elasticity of Schlemm's canal endothelial cells. *Biomech. Model. Mechanobiol.*, submitted for publication.
- Zhou, L., Maruyama, I., Li, Y., Cheng, E., Yue, B., 1999. Expression of integrin receptors in the human trabecular meshwork. *Curr. Eye Res.* 19, 395–402.